core protein in the liver of the mice may be unaffected by the knockout of the PA28γ gene.

Our results suggest that the interaction of HCV core protein with PA28γ leads to the activation of the *srebp-1c* promoter along an LXRα/RXRα-dependent pathway and the development of liver steatosis and HCC. HCV core protein was not included in the LXRα/RXRα–LXRE complex (Fig. 3*A*), suggesting that HCV core protein indirectly activates the *srebp-1c* promoter. Cytoplasmic HCV core protein was shown to interact with Sp110b, which is a transcriptional corepressor of RARα-dependent transcription, and this interaction leads to the sequestering of Sp110b in the cytoplasm, resulting in the activation of RARα-dependent transcription (29). The sequestration of an unidentified corepressor of the LXRα/RXRα heterodimer in the cytoplasm by HCV core protein may also contribute to the activation of the *srebp-1c* promoter. Although the precise physiological function of PA28γ-proteasome activity in the nucleus is not known, PA28γ has previously been shown (21) to regulate nuclear hormone receptors by means of the degradation of its coactivator SRC-3 and to participate in the fully Hsp90-dependent protein refolding (28). It appears reasonable to speculate that degradation or refolding of HCV core protein in a PA28γ-dependent pathway might be involved in the modulation of transcriptional regulators of various promoters, including the *srebp-1c* promoter. Saturated or monounsaturated fatty acids have been shown to enhance HCV RNA replication in Huh7 cells containing the full-length HCV replicon (7). The up-regulation of fatty acid biosynthesis by HCV core protein may also contribute to the efficient replication of HCV and to the progression of HCV pathogenesis.

Expression of HCV core protein was reported to enhance production of reactive oxygen species (ROS) (30), which leads to carbonylation of intracellular proteins (31). Enhancement of ROS production may trigger double-stranded DNA breaks and result in the development of HCC (30, 32, 33). HCV core protein could enhance the protein carbonylation in the liver of the transgenic mice in the presence but not in the absence of PA28γ (SI Fig. 7), suggesting that PA28γ is required for ROS production induced by HCV core protein. Development of HCC was observed in PA28γ$^{+/+}$CoreTg mice but not in PA28γ$^{-/-}$CoreTg mice (Table 1). Enhancement of ROS production by HCV core protein in the presence of PA28γ might be involved in the development of HCC in PA28γ$^{+/+}$CoreTg mice.

It is well known that resistant viruses readily emerge during the treatment with antiviral drugs targeting the viral protease or replicase, especially in the case of infection with RNA viruses. Therefore, antivirals targeting the host factors that are indispensable for the propagation of viruses might be an ideal target for the development of antiviral agents because of a lower rate of mutation than that of viral genome, if they have no side effects to patients. Importantly, the amino acid sequence of PA28γ of mice is identical to that of human, and mouse PA28γ is dispensable because PA28γ knockout mice exhibit no abnormal phenotype except for mild growth retardation. Therefore, PA28γ might be a promising target for an antiviral treatment of chronic hepatitis C with negligible side effects.

In summary, we observed that a knockout of the PA28γ gene from PA28γ$^{+/+}$CoreTg mice induced the accumulation of HCV core protein in the nucleus and disrupted the development of both steatosis and HCC. Activation of the *srebp-1c* promoter was up-regulated by HCV core protein both *in vitro* and *in vivo* through a PA28γ-dependent pathway, suggesting that PA28γ plays a crucial role in the development of liver pathology induced by HCV infection.

Materials and Methods

Histology and immunohistochemistry, real-time PCR, and detection of proteins modified by ROS are discussed in *SI Materials and Methods*.

Plasmids and Reagents. Human PA28γ cDNA was isolated from a human fetal brain library (18). The gene encoding HCV core protein was amplified from HCV strain J1 (genotype 1b) (34) and cloned into pCAG-GS (35). Mouse cDNAs of RXRα and LXRα were amplified by PCR from the total cDNAs of the mouse liver. The RXRα and LXRα genes were introduced into pEF-FLAGGspGBK (36) and pcDNA3.1 (Invitrogen, Carlsbad, CA), respectively. The targeting fragment for human PA28γ knockdown (GGATCCGGTGGATCAGGAAGTGAAGTTCAAGAGA-CTTCACTTCCTGATCCACCTTTTTTGGAAAAGCTT) was introduced into the BamHI and HindIII sites of pSilencer 4.1 U6 hygro vector (Ambion, Austin, TX). Mouse anti-FLAG (M2) and mouse anti-β-actin antibodies were purchased from Sigma (St. Louis, MO). Rabbit polyclonal antibody against synthetic peptides corresponding to amino acids 70–85 of PA28γ was obtained from AFFINITI (Exeter, U.K.). Horseradish peroxidase-conjugated goat anti-mouse and anti-rabbit IgGs were purchased from ICN Pharmaceuticals (Aurora, OH). Rabbit anti-HCV core protein was prepared by immunization with recombinant HCV core protein (amino acids 1-71), as described in ref. 24. Mouse monoclonal antibody to HCV core protein was kindly provided by S. Yagi (37). The plasmid for expression of HA-tagged ubiquitin was described in ref. 27.

Preparation of PA28γ-Knockout HCV CoreTg Mice. The generation of C57BL/6 mice carrying the gene encoding HCV core protein genotype 1b line C49 and that of PA28γ$^{-/-}$ mice have been reported previously (22, 25). Both strains were crossbred with each other to create PA28γ$^{-/-}$CoreTg mice. PA28γ$^{-/-}$CoreTg mice were identified by PCR targeted at the PA28γ or HCV core gene (22, 25). Using 1 μg of genomic DNA obtained from the mouse tail, the PA28γ gene was amplified by PCR with the following primers: sense, PA28-3 (AGGTGGATCAGGAAGTGAAGCTCAA); and antisense, PA28γ-5cr (CACCTCACTTGTGATCCGCTCTCT-GAAAGAATCAACC). The targeted sequence for the PA28γ-knockout mouse was detected by PCR using the PA28-3 primer and the PAKO-4 primer (TGCAGTTCATTCAGGGCACCGGA-CAG). The transgene encoding HCV core protein was detected by PCR as described in ref. 25. The expression of PA28γ and HCV core protein in the livers of 6-month-old mice was confirmed by Western blotting with mouse monoclonal antibody to HCV core protein, clone 11-10, and rabbit antibody to PA28γ. Mice were cared for according to the institutional guidelines. The mice were given ordinary feed, CRF-1 (Charles River Laboratories, Yokohama, Japan), and they were maintained under specific pathogen-free conditions.

All animal experiments conformed to the Guidelines for the Care and Use of Laboratory Animals, and they were approved by the Institutional Committee of Laboratory Animal Experimentation (Research Institute for Microbial Diseases, Osaka University).

Preparation of Mouse Embryonic Fibroblasts. MEFs were prepared as described in ref. 22. MEFs were cultured at 37°C under an atmosphere of 5% CO_2 in Dulbecco's modified Eagle's medium (Sigma) supplemented with 10% FBS, penicillin, streptomycin, sodium pyruvate, and nonessential amino acids.

Transfection and Immunoblotting. Plasmid vectors were transfected into the MEFs and 293T cells by liposome-mediated transfection by using Lipofectamine 2000 (Invitrogen). The amount of HCV core protein in the liver tissues was determined by an ELISA as described in ref. 37. The cell lysates were subjected to SDS/PAGE (12.5% gel), and they were then transferred onto PVDF membranes. Proteins on the membranes were treated with specific antibody and Super Signal Femto (Pierce, Rockford, IL). The results were then visualized by using an LAS3000 imaging system (Fuji Photo Film, Tokyo, Japan). The method of immunoprecipitation test is described in ref. 18.

Reporter Assay for *srebp-1c* Promoter Activity. The genomic DNA fragment encoding the *srebp-1c* promoter region (located from residues −410 to +24) was amplified from a mouse genome. The fragment was introduced into the KpnI and HindIII sites of pGL3-Basic (Promega, Madison, WI), and it was designated as pGL3-srebp-1cPro. The plasmids encoding RXRα and LXRα were transfected into MEFs together with pGL3-srebp-1cPro and a control plasmid encoding *Renilla* luciferase (Promega). The total DNA for transfection was normalized by the addition of empty plasmids. Cells were harvested at 24 h posttransfection. The ligand of RXRα, 9-*cis*-retinoic acid (Sigma), and that of LXRα, 22(*R*)-hydroxylcholesterol (Sigma) were added at a final concentration of 5 μM each to the culture medium of 293T cells transfected with pGL3-srebp-1cPro together with expression plasmids encoding RXRα, LXRα, and HCV core protein at 24 h posttransfection. Cells were harvested 24 h after treatment. Luciferase activity was measured by using the dual-luciferase reporter assay system (Promega). Firefly luciferase activity was standardized with that of *Renilla* luciferase, and the results are expressed as the fold increase in relative luciferase units.

Electrophoresis Mobility Shift Assay (EMSA). EMSA was carried out by using a LightShift Chemiluminescent EMSA kit (Pierce) according to the manufacturer's protocol. Nuclear extract of the cell lines and liver tissue was prepared with an NE-PER nuclear and cytoplasmic extraction reagent kit (Pierce). Briefly, double-stranded oligonucleotides for EMSA were prepared by annealing both strands of each LXRE of the *srebp-1c* promoter (5′-GGACGCCCGCTAGTAACCCCGGC-3′) (16). Both strands were labeled at the 5′ ends with biotin. The annealed probe was incubated for 20 min on ice with nuclear extract (3 μg of protein) in a reaction buffer containing 10 mM Tris·HCl (pH 7.5), 50 mM KCl, 1 mM DTT, 0.05 μg/μl poly(dI-dC), 2.5% glycerol, 0.05% Nonidet P-40, and 0.1 nM labeled probe, with or without 1 mM nonlabeled probe. The resulting mixture was subjected to PAGE (5% gel) at 120 V for 30 min in 0.5× TBE. The DNA–protein complex was transferred to a Hybond N+ membrane (Amersham, Piscataway, NJ), incubated with horseradish peroxidase-conjugated streptavidin, and visualized by using an LAS3000 imaging system.

Statistical Analysis. The results are expressed as the mean ± SD. The significance of differences in the means was determined by Student's *t* test.

We thank H. Murase for secretarial work and D. C. S. Huang for providing the plasmids. This work was supported in part by grants-in-aid from the Ministry of Health, Labor, and Welfare; the Ministry of Education, Culture, Sports, Science, and Technology; the 21st Century Center of Excellence Program; and the Foundation for Biomedical Research and Innovation.

1. Wasley A, Alter MJ (2000) *Semin Liver Dis* 20:1–16.
2. Bach N, Thung SN, Schaffner F (1992) *Hepatology* 15:572–577.
3. Lefkowitch JH, Schiff ER, Davis GL, Perrillo RP, Lindsay K, Bodenheimer HC, Jr., Balart LA, Ortego TJ, Payne J, Dienstag JL, *et al.* (1993) *Gastroenterology* 104:595–603.
4. Barba G, Harper F, Harada T, Kohara M, Goulinet S, Matsuura Y, Eder G, Schaff Z, Chapman MJ, Miyamura T, Brechot C (1997) *Proc Natl Acad Sci USA* 94:1200–1205.
5. Hope RG, McLauchlan J (2000) *J Gen Virol* 81:1913–1925.
6. Moriya K, Fujie H, Shintani Y, Yotsuyanagi H, Tsutsumi T, Ishibashi K, Matsuura Y, Kimura S, Miyamura T, Koike K (1998) *Nat Med* 4:1065–1067.
7. Kapadia SB, Chisari FV (2005) *Proc Natl Acad Sci USA* 102:2561–2566.
8. Su AI, Pezacki JP, Wodicka L, Brideau AD, Supekova L, Thimme R, Wieland S, Bukh J, Purcell RH, Schultz PG, Chisari FV (2002) *Proc Natl Acad Sci USA* 99:15669–15674.
9. Wang C, Gale M, Jr, Keller BC, Huang H, Brown MS, Goldstein JL, Ye J (2005) *Mol Cell* 18:425–434.
10. Horton JD, Shimomura I, Brown MS, Hammer RE, Goldstein JL, Shimano H (1998) *J Clin Invest* 101:2331–2339.
11. Pai JT, Guryev O, Brown MS, Goldstein JL (1998) *J Biol Chem* 273:26138–26148.
12. Shimano H, Horton JD, Hammer RE, Shimomura I, Brown MS, Goldstein JL (1996) *J Clin Invest* 98:1575–1584.
13. Shimano H, Horton JD, Shimomura I, Hammer RE, Brown MS, Goldstein JL (1997) *J Clin Invest* 99:846–854.
14. Shimano H, Shimomura I, Hammer RE, Herz J, Goldstein JL, Brown MS, Horton JD (1997) *J Clin Invest* 100:2115–2124.
15. Repa JJ, Liang G, Ou J, Bashmakov Y, Lobaccaro JM, Shimomura I, Shan B, Brown MS, Goldstein JL, Mangelsdorf DJ (2000) *Genes Dev* 14:2819–2830.
16. Yoshikawa T, Shimano H, Amemiya-Kudo M, Yahagi N, Hasty AH, Matsuzaka T, Okazaki H, Tamura Y, Iizuka Y, Ohashi K, *et al.* (2001) *Mol Cell Biol* 21:2991–3000.
17. Tsutsumi T, Suzuki T, Shimoike T, Suzuki R, Moriya K, Shintani Y, Fujie H, Matsuura Y, Koike K, Miyamura T (2002) *Hepatology* 35:937–946.
18. Moriishi K, Okabayashi T, Nakai K, Moriya K, Koike K, Murata S, Chiba T, Tanaka K, Suzuki R, Suzuki T, *et al.* (2003) *J Virol* 77:10237–10249.
19. Masson P, Andersson O, Petersen UM, Young P (2001) *J Biol Chem* 276:1383–1390.
20. Li J, Rechsteiner M (2001) *Biochimie* 83:373–383.
21. Li X, Lonard D, Jung SY, Malovannaya A, Feng Q, Qin J, Tsai SY, Tsai M, O'Malley BW (2006) *Cell* 124:381–392.
22. Murata S, Kawahara H, Tohma S, Yamamoto K, Kasahara M, Nabeshima Y, Tanaka K, Chiba T (1999) *J Biol Chem* 274:38211–38215.
23. Falcon V, Acosta-Rivero N, Chinea G, Gavilondo J, de la Rosa MC, Menendez I, Duenas-Carrera S, Vina A, Garcia W, Gra B, *et al.* (2003) *Biochem Biophys Res Commun* 305:1085–1090.
24. Suzuki R, Sakamoto S, Tsutsumi T, Rikimaru A, Tanaka K, Shimoike T, Moriishi K, Iwasaki T, Mizumoto K, Matsuura Y, *et al.* (2005) *J Virol* 79:1271–1281.
25. Moriya K, Yotsuyanagi H, Shintani Y, Fujie H, Ishibashi K, Matsuura Y, Miyamura T, Koike K (1997) *J Gen Virol* 78:1527–1531.
26. Yasui K, Wakita T, Tsukiyama-Kohara K, Funahashi SI, Ichikawa M, Kajita T, Moradpour D, Wands JR, Kohara M (1998) *J Virol* 72:6048–6055.
27. Suzuki R, Tamura K, Li J, Ishii K, Matsuura Y, Miyamura T, Suzuki T (2001) *Virology* 280:301–309.
28. Minami Y, Kawasaki H, Minami M, Tanahashi N, Tanaka K, Yahara I (2000) *J Biol Chem* 275:9055–9061.
29. Watashi K, Hijikata M, Tagawa A, Doi T, Marusawa H, Shimotohno K (2003) *Mol Cell Biol* 23:7498–7509.
30. Machida K, Cheng KT, Lai CK, Jeng KS, Sung VM, Lai MM (2006) *J Virol* 80:7199–7207.
31. Nystrom T (2005) *EMBO J* 24:1311–1317.
32. Bromberg JF, Wrzeszczynska MH, Devgan G, Zhao Y, Pestell RG, Albanese C, Darnell JE, Jr (1999) *Cell* 98:295–303.
33. Carballo M, Conde M, El Bekay R, Martin-Nieto J, Camacho MJ, Monteseirin J, Conde J, Bedoya FJ, Sobrino F (1999) *J Biol Chem* 274:17580–17586.
34. Aizaki H, Aoki Y, Harada T, Ishii K, Suzuki T, Nagamori S, Toda G, Matsuura Y, Miyamura T (1998) *Hepatology* 27:621–627.
35. Niwa H, Yamamura K, Miyazaki J (1991) *Gene* 108:193–199.
36. Huang DC, Cory S, Strasser A (1997) *Oncogene* 14:405–414.
37. Aoyagi K, Ohue C, Iida K, Kimura T, Tanaka E, Kiyosawa K, Yagi S (1999) *J Clin Microbiol* 37:1802–1808.

Moriishi *et al*. 10.1073/pnas.0607312104.

Supporting Information

Files in this Data Supplement:

SI Figure 6
SI Figure 7
SI Methods and Materials

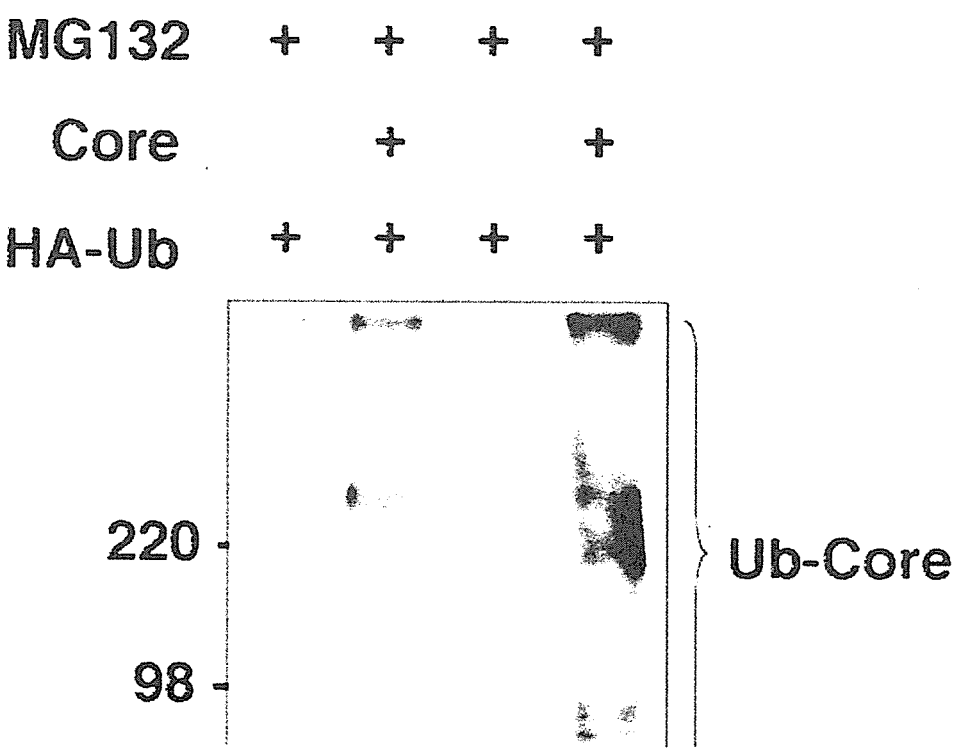

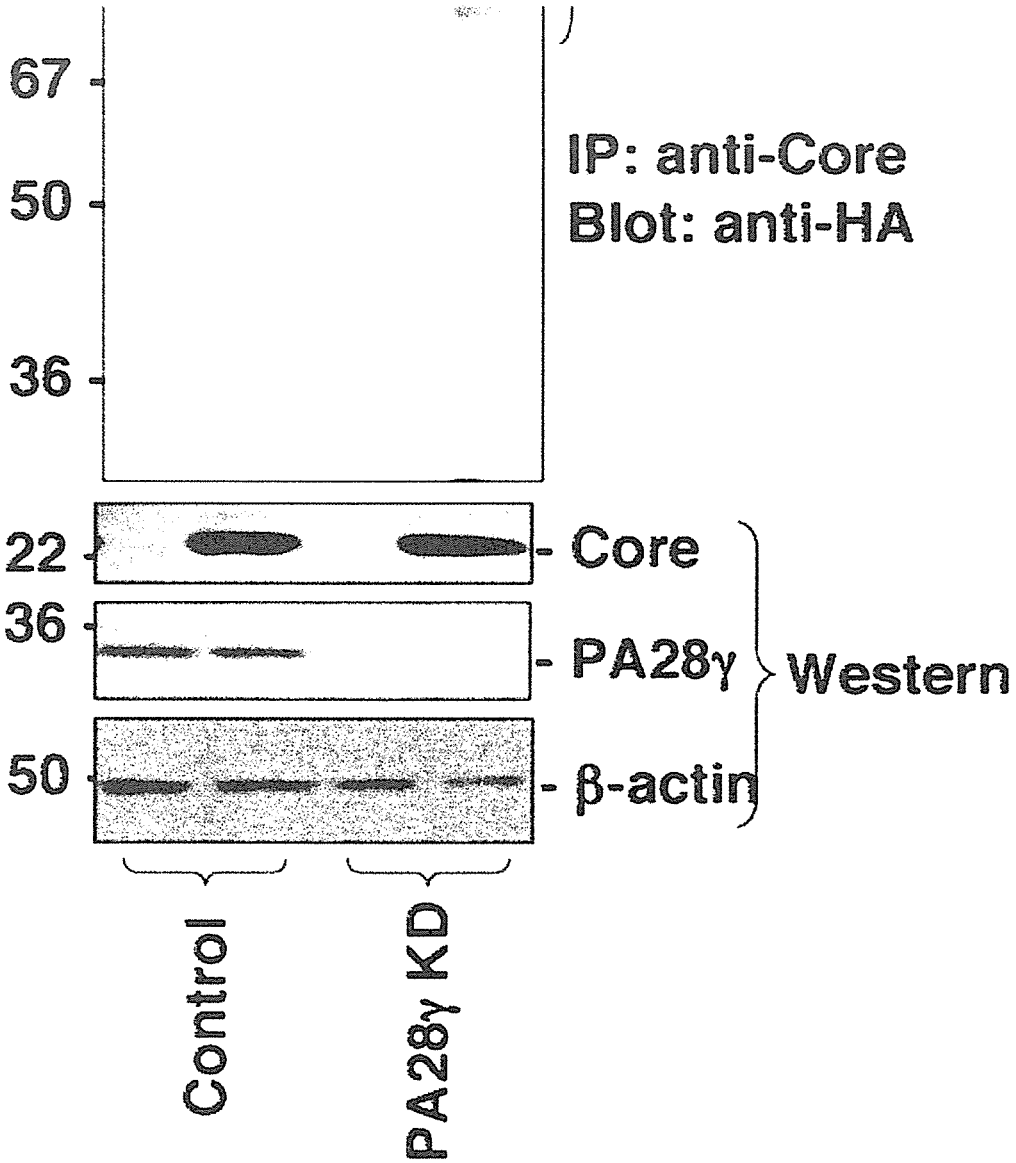

Fig. 6. Effect of PA28g knockdown on the ubiquitination of HCV core protein. HCV core protein was expressed with HA-tagged ubiquitin (HA-Ub) in the parental (Control) or PA28g-knockdown (PA28g KD) human hepatoma (FLC4) cells. The proteasome inhibitor MG132 was added to the culture supernatant at 24 h posttransfection to a final concentration of 10 mM. Cells were harvested at 36 h posttransfection, and cell lysates were subjected to immunoprecipitation (IP) with anti-core antibody and immunoblotting with anti-HA antibody (*Upper*). HCV core protein, PA28g, and b-actin in the cell lysate were detected by immunoblotting (*Lower*).

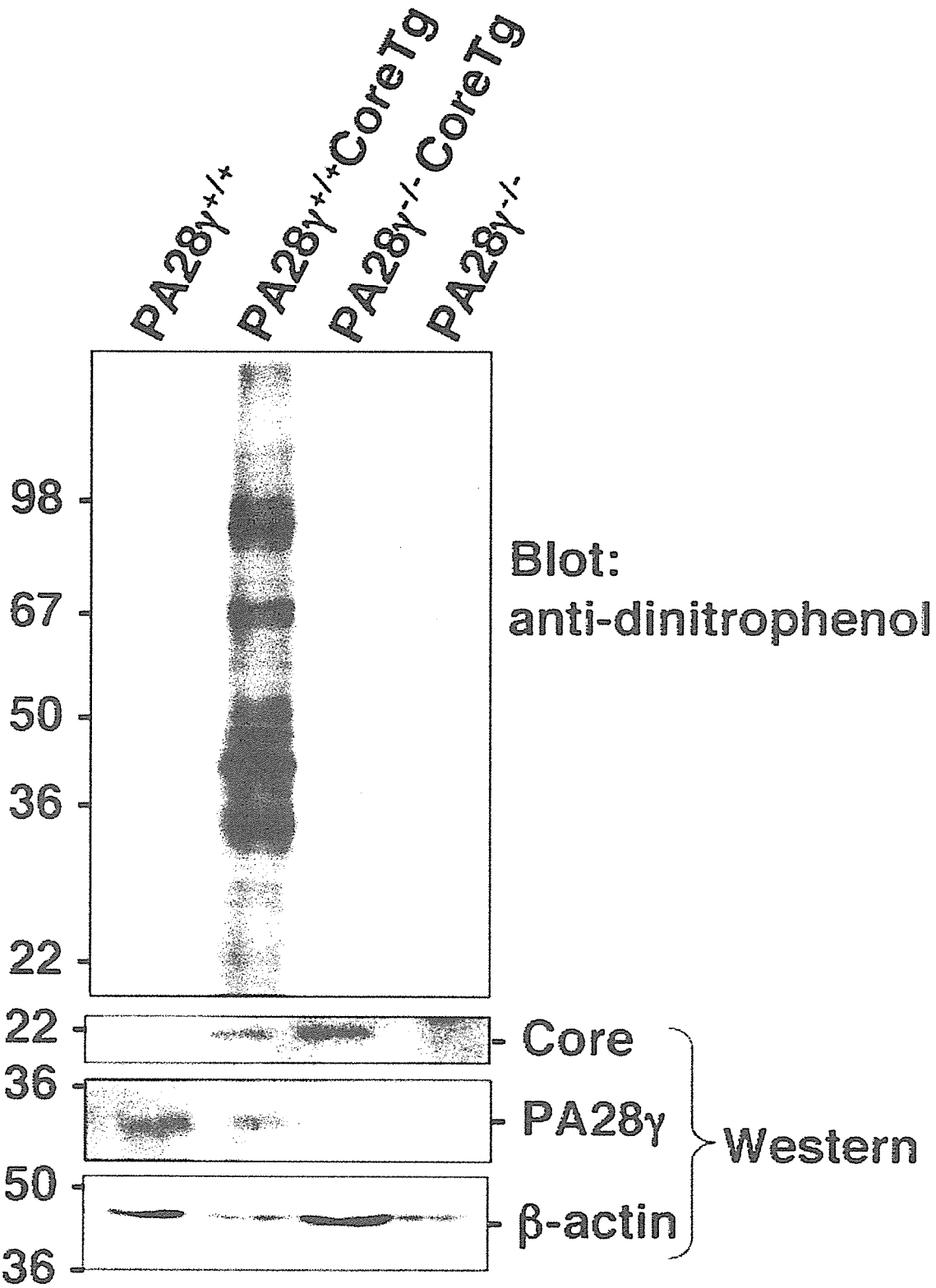

Fig. 7. Knockout of PA28g gene decreases the protein carbonylation induced by HCV core protein. Liver lysates were prepared from 6-month-old mice and subjected to OxyBlot assay. Each sample (20 mg of protein) was applied to a lane after the derivatization reaction (*Top*). HCV core protein, PA28g, and b-actin in the liver lysate were detected by immunoblotting (*Middle* and *Bottom*).

SI Methods and Materials

Histology and Immunohistochemistry. Formalin-fixed tissues were embedded in paraffin according to the standard procedures. Sections were stained with hematoxylin/eosin. To visualize lipids, frozen sections were stained with oil red O. For immunohistochemistry, sections of formalin-fixed tissues were treated with 3% (vol/vol) H_2O_2, washed twice with PBS, blocked with PBS containing 5% BSA, and incubated overnight with rabbit antibody to hepatitis C virus (HCV) core protein, followed by incubation with horseradish peroxidase-conjugated anti-rabbit IgG antibody (ICN, Aurora, OH) as a second antibody. Immunoreactive antigen was visualized with 3,3'-diaminobenzidine substrate. The percentage of the area occupied by oil red O-stained lipid droplets was calculated using Image-Pro software (MediaCybernetics, Silver Spring, MD). The area of the lipid droplets was examined in three different fields of every five randomly selected sections, and the areas were calculated by averaging 10 animals per genotype.

Real-Time PCR. RNA was prepared from the mouse livers with the use of TRIzol LS (Invitrogen, Carlsbad, CA). The first-strand cDNAs were synthesized with a first-strand cDNA synthesis kit (Amersham Pharmacia Biotech, Franklin Lakes, NJ). The amount of each cDNA was estimated by using Platinum SYBR Green qPCR super Mix UDG (Invitrogen) according to the manufacturer's protocol. The fluorescent signal was measured by using ABI prism 7000 (Applied Biosystems, Tokyo, Japan). The genes encoding mouse sterol regulatory element-binding proteins (SREBP)-1a, SREBP-1c, SREBP-2, stearoyl-CoA desaturase, acetyl-CoA carboxylase, fatty acid synthase, hydroxymethylglutaryl (HMG)-CoA synthase, HMG-CoA reductase, and hypoxanthine phosphoribosyltransferase were amplified with the primer pairs CACAGCGGTTTTGAACGAC and CTGGCTCCTCTTTGATCCCA, ACGGAGCCATGGATTGCACATTTG and TACATCTTTAAAGCAGCGGGTGCCGATGGT, ACCATTCTCCAGCAGTTCCGT and CCTCTCACAGTGACAGAAGGAGTT, TTCCCTCCTGCAAGCTCTAC and CGCAAGAAGGTGCTAACGAAC, GACAAACGAGTCTGGCTACT and TGATGAGTGACTGCCGAAAC, CTCCAAGACTGACTCGGCTACT and AGCTGGGAGCACATCTCGAA, GGTTGGAGTGTTCTCTTACGG and CTCTGACCAGATACCACGTTC, TATGCCCATCCCTGTTGGAG and CACGTGGAGTTTCTGTAGACGA, and CCAGCAAGCTTGCAACCTTAACCA and GTAATGATCAGTCAACGGGGGAC, respectively. The sense and antisense primers were located in different exons to avoid false-positive amplification from contaminated genomic DNA. Each PCR product was confirmed as a single band of the correct size by agarose gel electrophoresis (data not shown).

Detection of Proteins Modified by Reactive Oxygen Species. Carbonyl groups in proteins were detected by using an OxyBlot kit (Chemicon International, Temecula, CA) according to the manufacturer's instructions. The carbonyl groups in the side

chains of amino acid residues included in the protein are a hallmark of the oxidation status of proteins, and they are reacted with 2,4-dinitophenylhydrazine, resulting in the derivatization to 2,4-dinitrophenylhydrazone. The derivatized proteins are subjected to SDS/PAGE and Western blotting using the antibody to dinitrophenyl moiety.

JOURNAL OF VIROLOGY, Feb. 2007, p. 1727–1735 Vol. 81, No. 4
0022-538X/07/$08.00+0 doi:10.1128/JVI.01683-06

Involvement of the PA28γ-Dependent Pathway in Insulin Resistance Induced by Hepatitis C Virus Core Protein[▽]

Hironobu Miyamoto,[1] Kohji Moriishi,[1] Kyoji Moriya,[2] Shigeo Murata,[3] Keiji Tanaka,[3] Tetsuro Suzuki,[4] Tatsuo Miyamura,[4] Kazuhiko Koike,[2] and Yoshiharu Matsuura[1]*

Department of Molecular Virology, Research Institute for Microbial Diseases, Osaka University, Osaka,[1] Department of Internal Medicine, Graduate School of Medicine, University of Tokyo, Tokyo,[2] Department of Molecular Oncology, Tokyo Metropolitan Institute of Medical Science, Tokyo,[3] and Department of Virology II, National Institute of Infectious Diseases, Tokyo,[4] Japan

Received 4 August 2006/Accepted 16 November 2006

The hepatitis C virus (HCV) core protein is a component of nucleocapsids and a pathogenic factor for hepatitis C. Several epidemiological and experimental studies have suggested that HCV infection is associated with insulin resistance, leading to type 2 diabetes. We have previously reported that HCV core gene-transgenic (PA28γ$^{+/+}$CoreTg) mice develop marked insulin resistance and that the HCV core protein is degraded in the nucleus through a PA28γ-dependent pathway. In this study, we examined whether PA28γ is required for HCV core-induced insulin resistance in vivo. HCV core gene-transgenic mice lacking the PA28γ gene (PA28γ$^{-/-}$CoreTg) were prepared by mating of PA28γ$^{+/+}$CoreTg with PA28γ-knockout mice. Although there was no significant difference in the glucose tolerance test results among the mice, the insulin sensitivity in PA28γ$^{-/-}$CoreTg mice was recovered to a normal level in the insulin tolerance test. Tyrosine phosphorylation of insulin receptor substrate 1 (IRS1), production of IRS2, and phosphorylation of Akt were suppressed in the livers of PA28γ$^{+/+}$CoreTg mice in response to insulin stimulation, whereas they were restored in the livers of PA28γ$^{-/-}$CoreTg mice. Furthermore, activation of the tumor necrosis factor alpha promoter in human liver cell lines or mice by the HCV core protein was suppressed by the knockdown or knockout of the PA28γ gene. These results suggest that the HCV core protein suppresses insulin signaling through a PA28γ-dependent pathway.

Hepatitis C virus (HCV) is the causative agent in most cases of acute and chronic non-A, non-B hepatitis (15). Over one-half of patients with the acute infection evolve into a persistent carrier state (24). Chronic infection with HCV frequently induces hepatic steatosis, cirrhosis, and eventually hepatocellular carcinoma (22) and is known to be associated with diseases of extrahepatic organs, including an essential mixed cryoglobulinemia, porphyria cutanea tarda, membranoproliferative glomerulonephritis, and type 2 diabetes (13).

HCV is classified into the genus *Hepacivirus* of the family *Flaviviridae* and possesses a viral genome consisting of a single positive-strand RNA with a nucleotide length of about 9.5 kb. This viral genome encodes a single polyprotein composed of approximately 3,000 amino acids (9). The polyprotein is post-translationally cleaved by host cellular peptidases and viral proteases, resulting in 10 viral proteins (6, 10, 12). The HCV core protein is known to interact with viral-sense RNA of HCV to form the viral nucleocapsid (44). The HCV core protein is cleaved off at residue 191 by the host signal peptidase to release it from the E1 envelope protein and then by the host signal peptide peptidase at around amino acid residues 177 to 179 within the C-terminal transmembrane region (30, 39, 40). The mature core protein is retained mainly on the endoplasmic reticulum, although a portion moves to the nucleus and mitochondria (11, 51).

Recent epidemiological studies have indicated that type 2 diabetes is an HCV-associated disease (7, 29). However, it remains unclear how insulin resistance is induced in patients chronically infected with HCV, since there is no suitable model for investigating HCV pathogenesis. Type 2 diabetes is a complex, multisystemic disease with pathophysiology that includes a high level of hepatic glucose production and insulin resistance, which contribute to the development of hyperglycemia (8, 18). Although the precise mechanism by which these factors contribute to the induction of insulin resistance is difficult to understand, a high level of insulin production by pancreatic β cells under a state of insulin resistance is common in the development of type 2 diabetes. The hyperinsulinemia in the fasting state that is observed relatively early in type 2 diabetes is considered to be a secondary response that compensates for the insulin resistance (8, 18).

The HCV core protein is also known as a pathogenic factor that induces steatosis and hepatocellular carcinoma in mice (33, 35). Previously, we reported that insulin resistance occurs in HCV core gene-transgenic mice due at least partly to an increase in tumor necrosis factor alpha (TNF-α) secretion (47) and that the HCV core protein is degraded through a PA28γ/REGγ (11S regulator)-dependent pathway in the nucleus (32). It is well known that PA28γ enhances latent proteasome activity, although the biological significance of PA28γ is largely unknown, with the exception that PA28γ is known to regulate steroid receptor coactivator 3 (28). Although several reports suggested that the degradation of insulin receptor substrate (IRS) proteins by a ubiquitin-dependent proteasome activity contributes to insulin resistance (43, 50), the involvement of the HCV core protein in cooperation with PA28γ in the stability of IRS proteins and in the development of insulin resis-

* Corresponding author. Mailing address: Department of Molecular Virology, Research Institute for Microbial Diseases, Osaka University, 3-1 Yamadaoka, Suita, Osaka 565-0871, Japan. Phone: 81-6-6879-8340. Fax: 81-6-6879-8269. E-mail: matsuura@biken.osaka-u.ac.jp.

▽ Published ahead of print on 29 November 2006.

tance is not known. In this study, we examined the involvement of PA28γ in the induction of insulin resistance by the HCV core protein in vivo.

MATERIALS AND METHODS

Preparation of PA28γ-knockout HCV core gene-transgenic mice. C57BL/6 mice carrying the gene encoding HCV core protein genotype 1b ($PA28\gamma^{+/+}$ CoreTg) line C49 and $PA28\gamma^{-/-}$ mice have been described previously (35, 36). These two genotypes were crossbred to create $PA28\gamma^{+/-}$CoreTg mice. $PA28\gamma^{+/-}$CoreTg mice were bred to generate $PA28\gamma^{-/-}$CoreTg mice (35, 36). The HCV core gene and the target sequence to knock out the PA28γ gene were identified by PCR. The mice were given ordinary feed (CRF-1; Charles River Laboratories, Yokohama, Japan) and were maintained under specific-pathogen-free conditions.

Glucose tolerance test. The mice were fasted for more than 16 h before glucose administration. D-Glucose (1 g/kg body weight) was intraperitoneally administered to the mice. Blood samples were taken from the orbital sinus at the indicated time points. The plasma glucose concentration was measured by means of a MEDI-SAFE Mini blood glucose monitor (TERUMO, Tokyo, Japan). The serum insulin level was determined by a Mercodia (Uppsala, Sweden) ultrasensitive mouse insulin enzyme-linked immunosorbent assay (ELISA).

Insulin tolerance test. The mice were fed freely and then fasted during the study period. Human insulin (2 U/kg body weight) (Humulin; Eli Lilly, Indianapolis, IN) was intraperitoneally administered to the mice. The plasma glucose concentration was measured at the indicated time and was normalized based on the glucose concentration at the time just before insulin administration.

Histological analysis of pancreatic islets. Pancreas tissues were fixed with paraformaldehyde, embedded in paraffin, sectioned, and stained with hematoxylin and eosin. The relative islet area and islet number were determined with Image-Pro PLUS image analyzing software (NIPPON ROPER, Tokyo, Japan).

Estimation of tumor necrosis factor alpha and HCV core protein. Mouse TNF-α was measured by using a mouse TNF-α ELISA kit (Pierce, Rockford, IL) and normalized based on the amount of total protein in each sample. The protein concentration was estimated by using a BCA protein assay kit (Pierce). The amount of HCV core protein in the liver tissues was determined by using an ELISA system as described previously (4).

In vivo insulin stimulation and immunoblot analysis. Mice were fasted for more than 16 h before insulin stimulation and then anesthetized with ketamine and xylazine. Five units of insulin were injected into the mice via the interior vena cava. Livers of the mice were collected 5 min after the insulin injection and frozen in liquid nitrogen. Immunoblot analyses of the HCV core protein, PA28γ, and each of the insulin-signaling molecules were carried out with the liver tissue homogenates prepared in the homogenizing buffer containing 25 mM Tris-HCl (pH 7.4), 10 mM Na_3VO_4, 100 mM NaF, 50 mM $Na_4P_2O_7$, 10 mM EGTA, 10 mM EDTA, 2 mM phenylmethylsulfonyl fluoride, and 1% Nonidet P40 supplemented with Complete Protease Inhibitor Cocktail (Roche Diagnostics, Mannheim, Germany) (53). Tissue lysates were subjected to sodium dodecyl sulfate–2% to 15% gradient polyacrylamide gel electrophoresis (PAG Mini DAIICHI 2/15 13W; Daiichi Diagnostics, Tokyo, Japan) and electrotransferred onto polyvinylidene difluoride membranes (Immobilon-P; Millipore, Bedford, MA). The protein transferred onto the membrane was reacted with rabbit anti-HCV core (32), rabbit anti-Akt (Cell Signaling, Danvers, MA), rabbit anti-phospho-Ser473-Akt (Cell Signaling), rabbit anti-IRS1 (Upstate, Lake Placid, NY), rabbit anti-phospho-Tyr608 mouse insulin receptor substrate 1 (Sigma, St. Louis, MO), or rabbit anti-IRS2 (Upstate) polyclonal antibody and then incubated with horseradish peroxidase-conjugated anti-rabbit antibody. Blotted protein was visualized using Super Signal Femto (Pierce) and an LAS3000 imaging system (Fuji Photo Film, Tokyo, Japan).

Quantitative reverse transcription-PCR (RT-PCR). Total RNA was isolated from mouse liver using an RNeasy kit (QIAGEN, Valencia, CA). The RNA preparation was treated with a TURBO DNA-free kit (Ambion, Austin, TX) to remove DNA contamination in the samples. The first-strand cDNAs were synthesized by a first-strand cDNA synthesis kit (Amersham Biosciences, Franklin Lakes, NJ). The targeted cDNA was estimated by using Platinum SYBR Green qPCR Super Mix UDC (Invitrogen, Carlsbad, CA) according to the manufacturer's protocol. The fluorescent signal was measured by using an ABI Prism 7000 (Applied Biosystems, Foster City, CA). The genes encoding mouse TNF-α, IRS1, IRS2, and hypoxanthine phosphoribosyl transferase were amplified with the following primer pairs: 5′-GGTACAACCCATCGGCTGGCA-3′ (forward) and 5′-GCGACGTGGAACTGGCAGAAG-3′ (reverse) for TNF-α, 5′-ATAG CTCTGAGACCTTCTCAGCACCTAC-3′ (forward) and 5′-GGAGTTGCCCT CATTGCTGCCTAA-3′ (reverse) for IRS1, 5′-AGCCTGGGGATAATGGTG ACTATACCGA-3′ (forward) and 5′-TTGTGGGCAAAGGATGGGGACAC T-3′ (reverse) for IRS2, and 5′-CCAGCAAGCTTGCAACCTTAACCA-3′ (forward) and 5′-GTAATGATCAGTCAACGGGGGAC-3′ (reverse) for hypoxanthine phosphoribosyl transferase. Each PCR product was found as a single band with the correct size by agarose gel electrophoresis (data not shown).

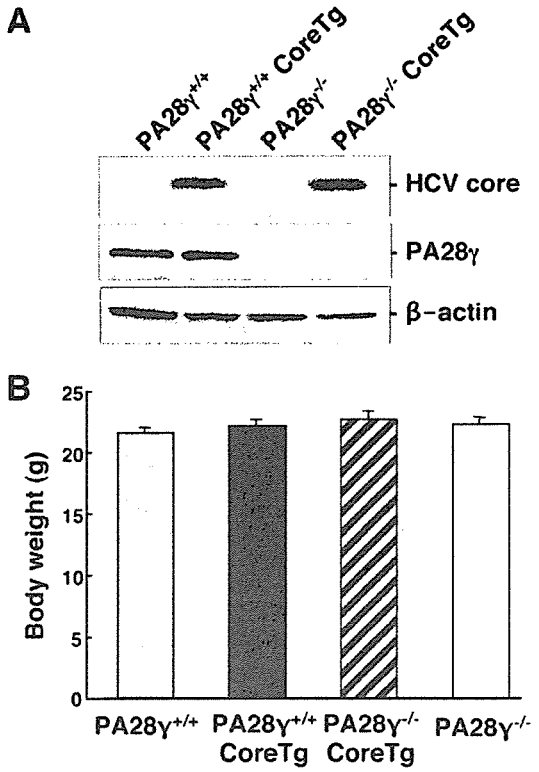

FIG. 1. Characterization of HCV core gene-transgenic mice deficient in the PA28γ gene. (A) Expression of the HCV core protein and PA28γ in the livers of $PA28\gamma^{+/+}$, $PA28\gamma^{+/+}$CoreTg, $PA28\gamma^{-/-}$, and $PA28\gamma^{-/-}$CoreTg mice. Lysates obtained from liver tissues of the mice (100 μg protein/lane) were subjected to sodium dodecyl sulfate-polyacrylamide gel electrophoresis and immunoblotting using antibodies to the HCV core protein, PA28γ, and β-actin. (B) Body weights of the mice. Body weights of 2-month-old mice were measured ($n = 7$ in each group). There were no statistically significant differences in body weights among the mice ($P > 0.05$).

Reporter assay for TNF-α promoter activity. The promoter region of the TNF-α gene (located from residues −1260 to +140) was amplified from mouse genomic DNA and was then introduced into the KpnI and BglII sites of pGL3-Basic (Promega, Madison, WI) (25). The resulting plasmid was designated as pGL3-tnf-aPro. The gene encoding the HCV core protein was amplified from HCV strain J1 (genotype 1b) and cloned into pCAG-GS (1, 38). To avoid contamination with endotoxin from *Escherichia coli*, the plasmid DNA was purified by using an EndoFree Plasmid Maxi kit (QIAGEN). The total amount of transfected DNA was normalized by the addition of empty plasmids. Plasmid vector was transfected into hepatoma cell lines by lipofection using Lipofectamine 2000 (Invitrogen). Cells were harvested at 24 h posttransfection. Luciferase activity was determined by using the Dual-Luciferase Reporter Assay system (Promega). Firefly luciferase activity was normalized to coexpressed *Renilla* luciferase activity. The amount of firefly luciferase activity was presented as the increase (n-fold) relative to the value for the sample lacking the HCV core protein, which was taken to be 1.0. PA28γ-knockdown cell lines were established by using pSilencer 2.1 U6 Hygro (Ambion) according to the manufacturer's protocol.

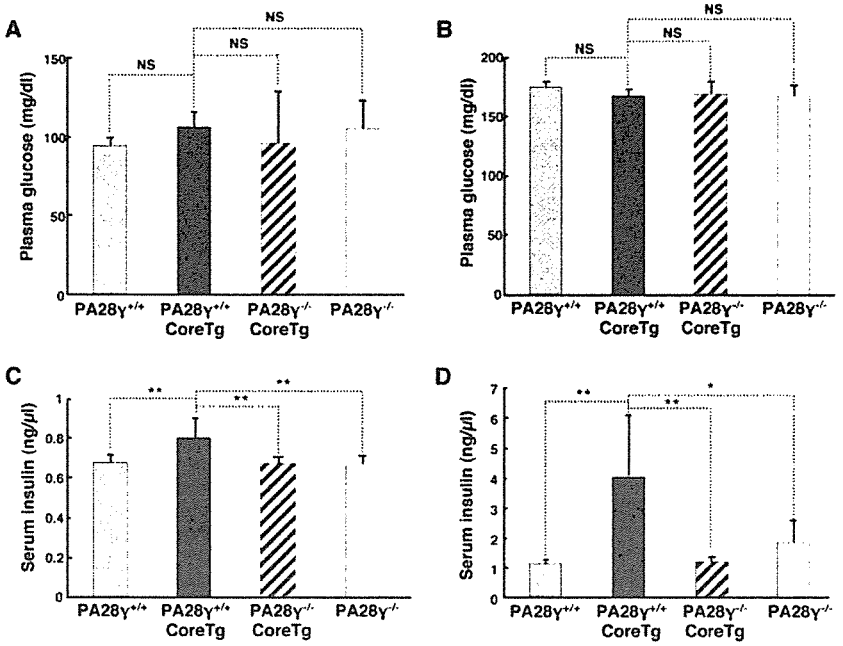

FIG. 2. Knockout of the PA28γ gene inhibited the hyperinsulinemia induced by HCV core protein. Plasma glucose levels of PA28$\gamma^{+/+}$, PA28$\gamma^{+/+}$CoreTg, PA28$\gamma^{-/-}$CoreTg, and PA28$\gamma^{-/-}$ mice under fasting (A) or fed (B) conditions ($n = 7$ in each group) are shown. Serum insulin levels in fasting (C) or fed (D) mice ($n = 7$ in each group) are also shown. Values are represented as means ± standard deviations. $*P < 0.05$; $**P < 0.01$. NS, not statistically significant.

Statistical analysis. The results are presented as means ± standard deviations. The significance of the differences was determined by Student's t test. P values of <0.05 were considered statistically significant.

RESULTS

HCV core gene-transgenic mice deficient in the PA28γ gene. To investigate the role of PA28γ in the development of insulin resistance in HCV core gene-transgenic (PA28$\gamma^{+/+}$CoreTg) mice, we generated HCV core gene-transgenic mice deficient in the PA28γ gene (PA28$\gamma^{-/-}$CoreTg). A PA28$\gamma^{+/+}$CoreTg mouse expressing an amount of PA28γ equal to that of its normal littermates (Fig. 1A) was crossbred with a PA28$\gamma^{-/-}$ mouse to generate a PA28$\gamma^{+/-}$ CoreTg mouse. PA28$\gamma^{+/-}$ CoreTg mice were bred with each other, and a PA28$\gamma^{-/-}$ CoreTg mouse was selected by PCR. The HCV core protein was expressed in PA28$\gamma^{+/+}$CoreTg and PA28$\gamma^{-/-}$CoreTg

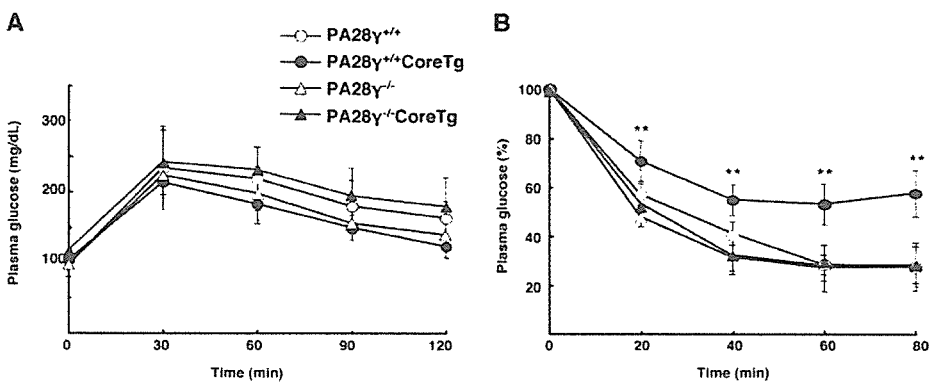

FIG. 3. Knockout of the PA28γ gene inhibits the insulin resistance induced by the HCV core protein. (A) Glucose tolerance test. D-Glucose was intraperitoneally administered to mice fasted for more than 16 h at 1 g/kg of body weight. Plasma glucose levels were estimated at the indicated times ($n = 5$ in each group). There were no significant differences in glucose levels among the mice ($P > 0.05$). (B) Insulin tolerance test. Human insulin (2 units/kg body weight) was intraperitoneally administered to the mice, and the plasma glucose levels were estimated at the indicated times. Values were normalized to the baseline glucose concentration at the time of insulin administration ($n = 5$ in each group). The values for the PA28$\gamma^{+/+}$ (open circles), PA28$\gamma^{+/+}$CoreTg (closed circles), PA28$\gamma^{-/-}$ (open triangles), and PA28$\gamma^{-/-}$CoreTg (closed triangles) mice are represented as means and ± standard deviations. Significant differences in insulin sensitivity ($P < 0.01$) in PA28$\gamma^{+/+}$CoreTg mice compared to that in PA28$\gamma^{+/+}$, PA28$\gamma^{-/-}$, or PA28$\gamma^{-/-}$CoreTg mice are indicated by double asterisks (**). There were no significant differences among PA28$\gamma^{+/+}$, PA28$\gamma^{-/-}$, and PA28$\gamma^{-/-}$CoreTg mice ($P > 0.05$).

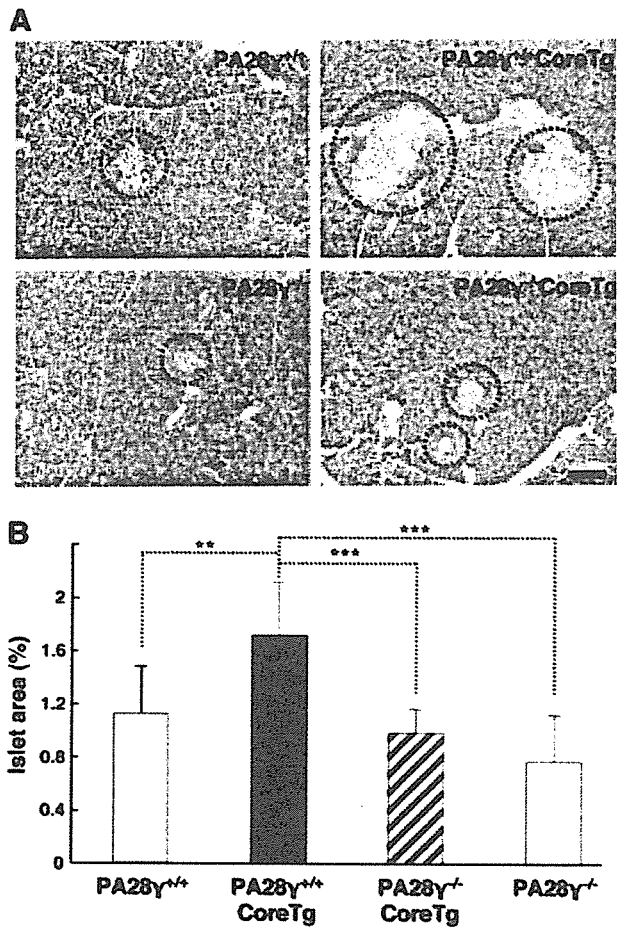

FIG. 4. PA28γ participated in the enlargement of pancreatic islets induced by the HCV core protein. (A) Histological sections prepared from pancreas tissues of PA28$\gamma^{+/+}$, PA28$\gamma^{+/+}$CoreTg, PA28$\gamma^{-/-}$, and PA28$\gamma^{-/-}$CoreTg mice were stained with hematoxylin and eosin. Dotted circles indicate pancreatic islets. (B) The area occupied by pancreatic islets was measured by computer software in three different fields of every six randomly selected sections of 10 mice per genotype and is represented as a percentage of the total pancreatic area. $**P < 0.01$; $***P < 0.001$. The scale bar indicates 100 μm.

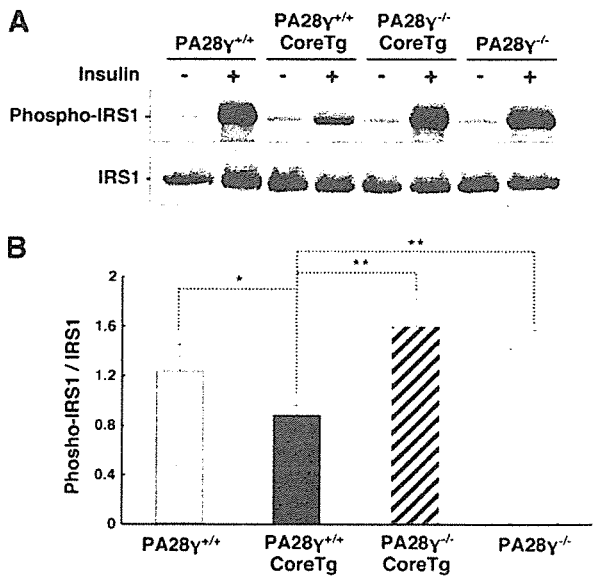

FIG. 5. PA28γ participated in the inhibition of the tyrosine phosphorylation of IRS1 induced by the HCV core protein. Liver tissues from PA28$\gamma^{+/+}$, PA28$\gamma^{+/+}$CoreTg, PA28$\gamma^{-/-}$, and PA28$\gamma^{-/-}$CoreTg mice were prepared after administration of insulin (+) or phosphate-buffered saline (−). The samples (100 μg of total protein) were examined by immunoblotting with antibodies against IRS1 and phospho-Tyr608 of mouse IRS1 (A). Phosphorylated IRS1 was estimated from the density on the immunoblotted membrane by using computer software (B) ($n = 5$ in each group). The data presented are representative of three independent experiments. $*P < 0.05$; $**P < 0.01$.

mice but not in PA28$\gamma^{+/+}$ (normal littermates) or PA28$\gamma^{-/-}$ mice. PA28γ was found at a similar level in PA28$\gamma^{+/+}$CoreTg and PA28$\gamma^{+/+}$ mice but was not present in either PA28$\gamma^{-/-}$ or PA28$\gamma^{-/-}$CoreTg mice (Fig. 1A). The expression of the HCV core protein in the livers of 2-month-old male mice was slightly higher in PA28$\gamma^{-/-}$CoreTg (1.36 ± 0.44 ng/mg of total protein; $n = 7$) than in PA28$\gamma^{+/+}$CoreTg (1.23 ± 0.22 ng/mg of total protein; $n = 7$) mice, but these values were not significantly different ($P > 0.05$). Insulin sensitivity is dependent on several conditions such as body weight, obesity, and liver steatosis (26). PA28$\gamma^{-/-}$ mice were slightly smaller than their normal littermates (PA28$\gamma^{+/+}$) at more than 3 months old, as described previously (36), but this was not significantly different in 2-month-old mice (Fig. 1B). PA28$\gamma^{+/+}$CoreTg mice exhibited severe hepatic steatosis from 4 months of age (35). To avoid the influence of hepatic steatosis and body weight on the examination of insulin resistance, 2-month-old mice were used in this study. Figure 1B shows the body weights of 2-month-old mice. There were no significant differences in body weight among PA28$\gamma^{+/+}$CoreTg, PA28$\gamma^{-/-}$CoreTg, PA28$\gamma^{-/-}$, and PA28$\gamma^{+/+}$ mice. Steatosis was not detected in the livers of the 2-month-old mice (data not shown).

PA28γ is involved in the development of hyperinsulinemia and insulin resistance in PA28$\gamma^{+/+}$CoreTg mice. In our previous study, we found a significant difference in serum insulin levels, but not in plasma glucose levels, between PA28$\gamma^{+/+}$ CoreTg mice and normal littermates (47). To determine the involvement of PA28γ in the development of insulin resistance in PA28$\gamma^{+/+}$CoreTg mice, we examined here the plasma glucose and insulin levels in the mice under fasting and fed conditions. Although no significant difference in plasma glucose levels was observed in the mice under either fasting (Fig. 2A) or fed (Fig. 2B) conditions, serum insulin levels were significantly higher in PA28$\gamma^{+/+}$CoreTg mice than in PA28$\gamma^{+/+}$ mice under both conditions (Fig. 2C and D), as described previously (47). In contrast, the serum insulin concentration in PA28$\gamma^{-/-}$CoreTg mice was recovered to a normal level similar to that of PA28$\gamma^{+/+}$ and PA28$\gamma^{-/-}$ mice under either fasting (Fig. 2C) or fed (Fig. 2D) conditions.

To determine the glucose intolerance among the mice, glucose was administered to the mice after fasting, and the plasma glucose level was then determined. There was no significant difference among the genotypes at any time point in the glucose tolerance test (Fig. 3A), suggesting that the volume of glucose was maintained at a normal level by the higher concentration of insulin in PA28$\gamma^{+/+}$CoreTg mice. In our previ-

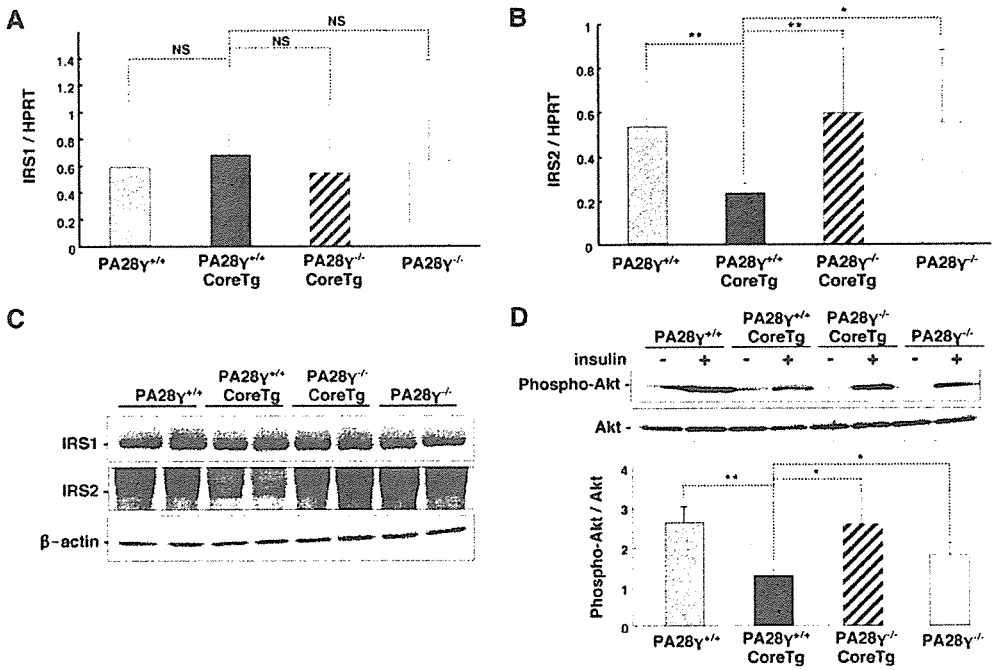

FIG. 6. PA28γ participated in the inhibition of the IRS2 expression and Akt phosphorylation induced by HCV core protein. The transcription of IRS1 (A) and IRS2 (B) was estimated by quantitative RT-PCR ($n = 5$ in each group). (C) The expression levels of IRS1 and IRS2 in the livers of the mice were determined by immunoblotting with specific antibodies. (D) Phosphorylation of Akt in the livers of the mice was examined by immunoblotting with antibodies against Akt and phosphorylated Akt. The ratio of Akt phosphorylation was determined by computer software based on the densities of phosphorylated Akt and a total amount of Akt ($n = 3$ in each group). The data presented are representative of three independent experiments. $*P < 0.05$; $**P < 0.01$. NS, not statistically significant; HPRT, hypoxanthine phosphoribosyl transferase.

ous study, the reduction in the plasma glucose concentration after insulin administration was impaired in PA28γ$^{+/+}$CoreTg mice (47). In this study, PA28γ$^{-/-}$CoreTg mice exhibited a normal insulin level comparable to those of PA28γ$^{+/+}$ and PA28γ$^{-/-}$ mice by an insulin tolerance test, in contrast to PA28γ$^{+/+}$CoreTg mice, in which a high concentration of plasma glucose was detected at all time points, as previously reported (Fig. 3B). These data suggest that hyperinsulinemia was induced in PA28γ$^{+/+}$CoreTg mice to compensate for insulin resistance and retain a physiological level of plasma glucose and that PA28γ participates in the development of hyperinsulinemia and insulin resistance in PA28γ$^{+/+}$CoreTg mice.

Morphology of pancreatic islets. Hyperinsulinemia and insulin resistance are expected to enlarge the pancreatic islet mass due to the overexpression of insulin. Our previous report showed the enlargement of the pancreatic islets in PA28γ$^{+/+}$ CoreTg mice. To clarify whether a knockout of the PA28γ gene restores the enlarged pancreatic islets to their normal size, the morphology of the pancreatic islets of the mice was evaluated by histologic examination (Fig. 4A). The relative islet area in the pancreatic cells of the PA28γ$^{-/-}$CoreTg mice was smaller than that of PA28γ$^{+/+}$CoreTg mice and comparable to that of PA28γ$^{+/+}$ and PA28γ$^{-/-}$ mice (Fig. 4B). Infiltration of inflammatory cells within or surrounding the islets was not found in all genotypes of mice. These results suggest that PA28γ also participates in the enlargement of pancreatic islets induced in PA28γ$^{+/+}$CoreTg mice.

PA28γ impairs the insulin-signaling pathway through the suppression of both tyrosine phosphorylation of IRS1 and expression of IRS2. Insulin binds to insulin receptors, resulting in the activation of downstream signaling (26). The activated insulin receptors phosphorylate themselves, IRS1, and IRS2. Phosphorylated IRS1 and IRS2 can activate phosphatidylinositol 3 (PI3)-kinase signaling, leading to the activation of glucose metabolism and cell growth. Our previous report showed that tyrosine phosphorylation of IRS1 is suppressed in the livers of PA28γ$^{+/+}$CoreTg mice and that the administration of anti-TNF-α antibody restores insulin sensitivity (47). We examined whether a knockout of the PA28γ gene could restore the tyrosine phosphorylation of IRS1. Tyrosine phosphorylation of IRS1 was suppressed in the livers of PA28γ$^{+/+}$ CoreTg mice in response to insulin stimulation, whereas it was recovered in PA28γ$^{-/-}$CoreTg mice to levels comparable to those in PA28γ$^{+/+}$and PA28γ$^{-/-}$ mice (Fig. 5).

Chronic hyperinsulinemia downregulates the expression of IRS2, which is one of the essential components of the insulin-signaling pathway in the liver (46). However, in our previous study, we showed that there was no significant difference in the phosphorylation of IRS2 between PA28γ$^{+/+}$CoreTg mice and their normal littermates (47). To gain more insight into the mechanisms of regulation of IRS expression, we determined the transcription and translation of IRS1 and IRS2 in the livers of the mice by real-time PCR and Western blotting, respectively. Although there was no significant difference in IRS1 expression at either the transcriptional or translational level among the mice

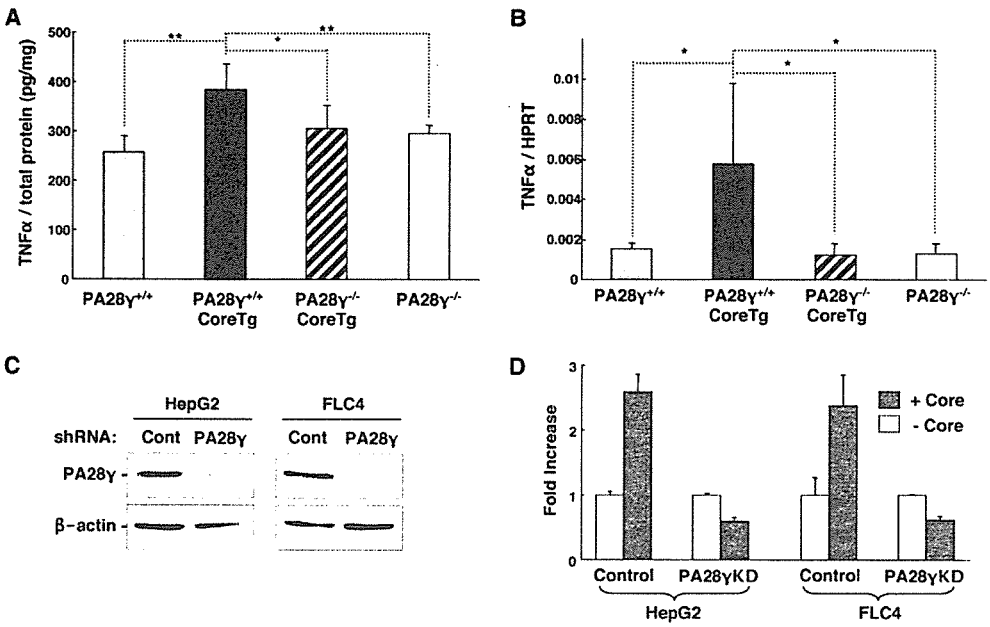

FIG. 7. PA28γ was required for activation of the TNF-α promoter by the HCV core protein. (A) Expression of TNF-α in the livers of mice was determined by ELISA (n = 5 in each group). (B) TNF-α mRNA in the livers of mice was examined by quantitative RT-PCR (n = 5 in each group). (C) Knockdown of the expression of PA28γ in the HepG2 and FLC-4 cell lines by the introduction of a plasmid encoding a short hairpin RNA (shRNA) targeted to the PA28γ gene. The expression levels of PA28γ and β-actin were determined by immunoblotting with specific antibodies. (D) Promoter activity of TNF-α in the presence or absence of the HCV core protein was determined by luciferase assay in the PA28γ-knockdown and control cell lines. The data presented are representative of three independent experiments. HPRT, hypoxanthine phosphoribosyl transferase.

(Fig. 6A and C), the expression of IRS2 was clearly impaired in PA28γ$^{+/+}$CoreTg mice at both the transcriptional and translational levels compared with that in other mice (Fig. 6B and C). The serine/threonine protein kinase Akt is phosphorylated by phosphoinositide-dependent kinase 1 (PDK1) under the activated condition of IRS family proteins (26). The insulin-induced phosphorylation of Akt was suppressed in the livers of PA28γ$^{+/+}$ CoreTg mice but not in those of PA28γ$^{+/+}$, PA28γ$^{-/-}$, or PA28γ$^{-/-}$CoreTg mice (Fig. 6D). These results suggest that the expression of the HCV core protein in the livers of mice in the presence of PA28γ impairs the insulin-signaling pathway through the suppression of both the tyrosine phosphorylation of IRS1 and the expression of IRS2.

PA28γ is required for activation of the TNF-α promoter by HCV core protein. TNF-α is an adipokine (54) and suppresses the signaling pathway of IRS1 and IRS2 (14, 42). Several reports suggested that the serum TNF-α level is higher in HCV patients than in healthy individuals (19, 37). Elevations of TNF-α levels have also been demonstrated in the livers of PA28γ$^{+/+}$CoreTg mice (47). To determine the involvement of PA28γ in the enhancement of TNF-α expression, the expression of TNF-α in the livers of each genotype was determined by ELISA and real-time PCR (Fig. 7A and B). Transcription and translation of TNF-α were increased in the livers of PA28γ$^{+/+}$ CoreTg mice but were restored in the livers of PA28γ$^{-/-}$ CoreTg mice to levels comparable to those of PA28γ$^{+/+}$ and PA28γ$^{-/-}$ mice. To determine the effect of PA28γ expression on the promoter activity of TNF-α in human liver cells, PA28γ-knockdown human hepatoma cell lines HepG2 and FLC4 were established by the introduction of a plasmid encoding a short hairpin RNA targeting the PA28γ gene in the cell lines. The expression of PA28γ was clearly suppressed in the cell lines (Fig. 7C). The expression of HCV core protein in the hepatoma cell lines potentiated TNF-α promoter activity, whereas the promoter activation by the HCV core protein was suppressed in the PA28γ-knockdown cell lines (Fig. 7D). These results suggest that PA28γ is required for the activation of the TNF-α promoter induced by the expression of the HCV core protein in human hepatoma cell lines.

DISCUSSION

HCV infection has a close association with type 2 diabetes, which is a polygenic disease with a pathophysiology that includes a defect in insulin secretion, increased hepatic glucose production, and resistance to the action of insulin (2, 8, 18). Insulin binds to insulin receptors, which exhibit tyrosine kinase activity, leading to the autophosphorylation and phosphorylation of IRS (56). Tyrosine phosphorylation in IRS proteins leads to the interaction between IRS proteins and the regulatory subunit p85 of PI3-kinase, which enhances glucose uptake and inhibits lypolysis (21). Activated PI3-kinase phosphorylates phosphatidylinositol 4,5-biphosphate to produce phosphatidylinositol 3,4,5-triphosphate, which contributes to the activation of PDK1 (55). Activated PDK1 phosphorylates downstream substrates including Akt and other kinases (55). A diabetic phenotype that included insulin resistance was found in IRS2-knockout mice with normal growth (57), although a

knockout of the IRS1 gene has been shown to lead to growth retardation and insulin resistance but not overt diabetes (5, 52). The double knockdown of IRS1 and IRS2 genes in the liver induces hyperinsulinemia and insulin resistance in mice (53). The reduction of both IRS1 and IRS2 under conditions of insulin resistance and hyperinsulinemia (3) and in the livers of *ob/ob* mice, an obese diabetic mouse model (20), has been reported previously. In the present study, the expression of the HCV core protein reduced the phosphorylation of tyrosine on IRS1 and the production of IRS2 in the livers of mice but did not completely abolish the activities of these genes, suggesting that residual activities of IRS transfer a faint signal to the downstream region of IRS. Therefore, PA28γ$^{+/+}$CoreTg mice may exhibit a milder phenotype than IRS1- and/or IRS2-knockout mice. In this study, knockout of the PA28γ gene restored the insulin sensitivity and signaling of IRS1 and IRS2 in PA28γ$^{+/+}$CoreTg mice, suggesting that the expression of the HCV core protein leads to the dysfunction of both IRS1 and IRS2 through a PA28γ-dependent pathway.

Our previous study suggested that the induction of TNF-α by the HCV core protein plays a role in insulin resistance (47). An increase in TNF-α levels has been correlated with obesity and insulin resistance in animal models and humans (14, 42). However, the mechanism by which TNF-α induces insulin resistance is not completely known. The expression of TNF-α has been shown to be increased in PA28γ$^{+/+}$CoreTg mice, resulting in the suppression of phosphorylation of IRS1, and insulin sensitivity in PA28γ$^{+/+}$CoreTg was improved by the administration of an anti-TNF-α antibody (47). In the present study, the expression level of TNF-α in PA28γ$^{-/-}$CoreTg mice was similar to that in PA28γ$^{-/-}$ mice or their normal littermates. The expression of the HCV core protein enhanced the promoter activity of the TNF-α gene in human liver cell lines but not in those with a knockdown of the PA28γ gene by RNA interference (Fig. 7D). These data suggest that PA28γ plays a crucial role in HCV core-induced expression of TNF-α. Sterol regulatory element-binding proteins (SREBPs) were shown to be increased at the stage of viremia in HCV-infected chimpanzees (49). SREBPs are known to regulate not only the biosynthesis of lipid but also the transcription of IRS2 and TNF-α (17, 45). Therefore, it might be feasible to speculate that the HCV core protein may cooperate with PA28γ to regulate the expression of SREBPs.

Houstis et al. previously reported that reactive oxygen species (ROS) are increased in both cellular and mouse models of insulin resistance induced by treatment with TNF-α or dexamethasone and that insulin sensitivity was restored by treatment with small antioxidant molecules (16). The HCV core protein potentiates ROS production in hepatoma cells and HCV core gene-transgenic mice (23, 34, 41). Accelerated production of ROS results in mitochondrion dysfunction, which contributes to a decrease in fatty acid oxidation. Defects in mitochondrial fatty acid oxidation enhance the production of intracellular fatty acyl coenzyme A (CoA) and diacylglycerol (48, 58). Mitochondrion dysfunction and accumulation of lipid droplets in mice expressing the HCV core or the full-length HCV polyprotein have been reported (27, 34). An increase in lipid droplets also leads to the accumulation of fatty acid CoA and diacylglycerol (48, 58). Fatty acyl CoA and diacylglycerol nonspecifically activate the Ser/Thr kinase cascade, leading to the enhancement of the serine phosphorylation of IRS1 (26). Serine phosphorylation on IRS1 blocks the tyrosine phosphorylation of IRS1 by insulin receptors (26). In the present study, however, serine phosphorylation of IRS1 in PA28γ$^{+/+}$ CoreTg mice was similar to that in PA28γ$^{-/-}$CoreTg mice (data not shown). TNF-α signaling pathways other than the accumulation of ROS and fatty acid intermediates may also participate in the inhibition of tyrosine phosphorylation on IRS1 in PA28γ$^{+/+}$ CoreTg mice.

How does the HCV core protein induce TNF-α production? Our previous report suggests that the HCV core protein is degraded through a PA28γ-dependent pathway (32). Recently, PA28γ has been shown to participate in the proteasome-dependent degradation of steroid receptor coactivator 3 (28). Degradation products of the HCV core protein via the PA28γ-dependent pathway may regulate the promoter activity of the TNF-α gene. PA28 proteins are necessary and sufficient to fully reconstitute Hsp90-initiated refolding together with Hsc70 and Hsp40 (31). Therefore, it might also be feasible to speculate that the HCV core protein refolded by an Hsp90/PA28γ-dependent pathway activates the promoter of the TNF-α gene together with an unknown transcription factor(s) or regulator(s).

In conclusion, the data obtained in this study suggest that the expression of the HCV core protein enhances the production of TNF-α and suppresses the phosphorylation of tyrosine on IRS1 and the production of IRS2 through a PA28γ-dependent pathway, thereby leading to insulin resistance. PA28γ may be a novel target for the treatment of HCV-induced diabetes.

ACKNOWLEDGMENTS

We gratefully thank H. Murase for secretarial work.

This study was supported in part by grants-in-aid from the Ministry of Health, Labor, and Welfare; the Ministry of Education, Culture, Sports, Science, and Technology; the Program for the Promotion of Fundamental Studies in Health Sciences of the National Institute of Biomedical Innovation (NIBIO); the 21st Century Center of Excellence Program; and the Foundation for Biomedical Research and Innovation.

REFERENCES

1. **Aizaki, H., Y. Aoki, T. Harada, K. Ishii, T. Suzuki, S. Nagamori, G. Toda, Y. Matsuura, and T. Miyamura.** 1998. Full-length complementary DNA of hepatitis C virus genome from an infectious blood sample. Hepatology **27:** 621–627.
2. **Allison, M. E., T. Wreghitt, C. R. Palmer, and G. J. Alexander.** 1994. Evidence for a link between hepatitis C virus infection and diabetes mellitus in a cirrhotic population. J. Hepatol. **21:**1135–1139.
3. **Anai, M., M. Funaki, T. Ogihara, J. Terasaki, K. Inukai, H. Katagiri, Y. Fukushima, Y. Yazaki, M. Kikuchi, Y. Oka, and T. Asano.** 1998. Altered expression levels and impaired steps in the pathway to phosphatidylinositol 3-kinase activation via insulin receptor substrates 1 and 2 in Zucker fatty rats. Diabetes **47:**13–23.
4. **Aoyagi, K., C. Ohue, K. Iida, T. Kimura, E. Tanaka, K. Kiyosawa, and S. Yagi.** 1999. Development of a simple and highly sensitive enzyme immunoassay for hepatitis C virus core antigen. J. Clin. Microbiol. **37:**1802–1808.
5. **Araki, E., M. A. Lipes, M. E. Patti, J. C. Bruning, B. Haag III, R. S. Johnson, and C. R. Kahn.** 1994. Alternative pathway of insulin signalling in mice with targeted disruption of the IRS-1 gene. Nature **372:**186–190.
6. **Bukh, J., R. H. Purcell, and R. H. Miller.** 1994. Sequence analysis of the core gene of 14 hepatitis C virus genotypes. Proc. Natl. Acad. Sci. USA **91:**8239–8243.
7. **Caronia, S., K. Taylor, L. Pagliaro, C. Carr, U. Palazzo, J. Petrik, S. O'Rahilly, S. Shore, B. D. Tom, and G. J. Alexander.** 1999. Further evidence for an association between non-insulin-dependent diabetes mellitus and chronic hepatitis C virus infection. Hepatology **30:**1059–1063.
8. **Cavaghan, M. K., D. A. Ehrmann, and K. S. Polonsky.** 2000. Interactions between insulin resistance and insulin secretion in the development of glucose intolerance. J. Clin. Investig. **106:**329–333.
9. **Choo, Q. L., G. Kuo, A. J. Weiner, L. R. Overby, D. W. Bradley, and M. Houghton.** 1989. Isolation of a cDNA clone derived from a blood-borne non-A, non-B viral hepatitis genome. Science **244:**359–362.

10. **Choo, Q. L., K. H. Richman, J. H. Han, K. Berger, C. Lee, C. Dong, C. Gallegos, D. Coit, R. Medina-Selby, P. J. Barr, et al.** 1991. Genetic organization and diversity of the hepatitis C virus. Proc. Natl. Acad. Sci. USA **88**:2451–2455.
11. **Falcon, V., N. Acosta-Rivero, G. Chinea, J. Gavilondo, M. C. de la Rosa, I. Menendez, S. Duenas-Carrera, A. Vina, W. Garcia, B. Gra, M. Noa, E. Reytor, M. T. Barcelo, F. Alvarez, and J. Morales-Grillo.** 2003. Ultrastructural evidences of HCV infection in hepatocytes of chronically HCV-infected patients. Biochem. Biophys. Res. Commun. **305**:1085–1090.
12. **Grakoui, A., D. W. McCourt, C. Wychowski, S. M. Feinstone, and C. M. Rice.** 1993. Characterization of the hepatitis C virus-encoded serine proteinase: determination of proteinase-dependent polyprotein cleavage sites. J. Virol. **67**:2832–2843.
13. **Gumber, S. C., and S. Chopra.** 1995. Hepatitis C: a multifaceted disease. Review of extrahepatic manifestations. Ann. Intern. Med. **123**:615–620.
14. **Hotamisligil, G. S.** 1999. The role of TNFalpha and TNF receptors in obesity and insulin resistance. J. Intern. Med. **245**:621–625.
15. **Houghton, M., A. Weiner, J. Han, G. Kuo, and Q. L. Choo.** 1991. Molecular biology of the hepatitis C viruses: implications for diagnosis, development and control of viral disease. Hepatology **14**:381–388.
16. **Houstis, N., E. D. Rosen, and E. S. Lander.** 2006. Reactive oxygen species have a causal role in multiple forms of insulin resistance. Nature **440**:944–948.
17. **Ide, T., H. Shimano, N. Yahagi, T. Matsuzaka, M. Nakakuki, T. Yamamoto, Y. Nakagawa, A. Takahashi, H. Suzuki, H. Sone, H. Toyoshima, A. Fukamizu, and N. Yamada.** 2004. SREBPs suppress IRS-2-mediated insulin signalling in the liver. Nat. Cell Biol. **6**:351–357.
18. **Kahn, B. B.** 1998. Type 2 diabetes: when insulin secretion fails to compensate for insulin resistance. Cell **92**:593–596.
19. **Kallinowski, B., K. Haseroth, G. Marinos, C. Hanck, W. Stremmel, L. Theilmann, M. V. Singer, and S. Rossol.** 1998. Induction of tumour necrosis factor (TNF) receptor type p55 and p75 in patients with chronic hepatitis C virus (HCV) infection. Clin. Exp. Immunol. **111**:269–277.
20. **Kerouz, N. J., D. Horsch, S. Pons, and C. R. Kahn.** 1997. Differential regulation of insulin receptor substrates-1 and -2 (IRS-1 and IRS-2) and phosphatidylinositol 3-kinase isoforms in liver and muscle of the obese diabetic (ob/ob) mouse. J. Clin. Investig. **100**:3164–3172.
21. **Kido, Y., J. Nakae, and D. Accili.** 2001. Clinical review 125: the insulin receptor and its cellular targets. J. Clin. Endocrinol. Metab. **86**:972–979.
22. **Kiyosawa, K., T. Sodeyama, E. Tanaka, Y. Gibo, K. Yoshizawa, Y. Nakano, S. Furuta, Y. Akahane, K. Nishioka, R. H. Purcell, et al.** 1990. Interrelationship of blood transfusion, non-A, non-B hepatitis and hepatocellular carcinoma: analysis by detection of antibody to hepatitis C virus. Hepatology **12**:671–675.
23. **Korenaga, M., T. Wang, Y. Li, L. A. Showalter, T. Chan, J. Sun, and S. A. Weinman.** 2005. Hepatitis C virus core protein inhibits mitochondrial electron transport and increases reactive oxygen species (ROS) production. J. Biol. Chem. **280**:37481–37488.
24. **Kuo, G., Q. L. Choo, H. J. Alter, G. L. Gitnick, A. G. Redeker, R. H. Purcell, T. Miyamura, J. L. Dienstag, M. J. Alter, C. E. Stevens, et al.** 1989. An assay for circulating antibodies to a major etiologic virus of human non-A, non-B hepatitis. Science **244**:362–364.
25. **Kuprash, D. V., I. A. Udalova, R. L. Turetskaya, D. Kwiatkowski, N. R. Rice, and S. A. Nedospasov.** 1999. Similarities and differences between human and murine TNF promoters in their response to lipopolysaccharide. J. Immunol. **162**:4045–4052.
26. **Lazar, D. F., and A. R. Saltiel.** 2006. Lipid phosphatases as drug discovery targets for type 2 diabetes. Nat. Rev. Drug Discov. **5**:333–342.
27. **Lerat, H., M. Honda, M. R. Beard, K. Loesch, J. Sun, Y. Yang, M. Okuda, R. Gosert, S. Y. Xiao, S. A. Weinman, and S. M. Lemon.** 2002. Steatosis and liver cancer in transgenic mice expressing the structural and nonstructural proteins of hepatitis C virus. Gastroenterology **122**:352–365.
28. **Li, X., D. M. Lonard, S. Y. Jung, A. Malovannaya, Q. Feng, J. Qin, S. Y. Tsai, M. J. Tsai, and B. W. O'Malley.** 2006. The SRC-3/AIB1 coactivator is degraded in a ubiquitin- and ATP-independent manner by the REGgamma proteasome. Cell **124**:381–392.
29. **Mason, A. L., J. Y. Lau, N. Hoang, K. Qian, G. J. Alexander, L. Xu, L. Guo, S. Jacob, F. G. Regenstein, R. Zimmerman, J. E. Everhart, C. Wasserfall, N. K. Maclaren, and R. P. Perrillo.** 1999. Association of diabetes mellitus and chronic hepatitis C virus infection. Hepatology **29**:328–333.
30. **McLauchlan, J., M. K. Lemberg, G. Hope, and B. Martoglio.** 2002. Intramembrane proteolysis promotes trafficking of hepatitis C virus core protein to lipid droplets. EMBO J. **21**:3980–3988.
31. **Minami, Y., H. Kawasaki, M. Minami, N. Tanahashi, K. Tanaka, and I. Yahara.** 2000. A critical role for the proteasome activator PA28 in the Hsp90-dependent protein refolding. J. Biol. Chem. **275**:9055–9061.
32. **Moriishi, K., T. Okabayashi, K. Nakai, K. Moriya, K. Koike, S. Murata, T. Chiba, K. Tanaka, R. Suzuki, T. Suzuki, T. Miyamura, and Y. Matsuura.** 2003. Proteasome activator PA28γ-dependent nuclear retention and degradation of hepatitis C virus core protein. J. Virol. **77**:10237–10249.
33. **Moriya, K., H. Fujie, Y. Shintani, H. Yotsuyanagi, T. Tsutsumi, K. Ishibashi, Y. Matsuura, S. Kimura, T. Miyamura, and K. Koike.** 1998. The core protein of hepatitis C virus induces hepatocellular carcinoma in transgenic mice. Nat. Med. **4**:1065–1067.
34. **Moriya, K., K. Nakagawa, T. Santa, Y. Shintani, H. Fujie, H. Miyoshi, T. Tsutsumi, T. Miyazawa, K. Ishibashi, T. Horie, K. Imai, T. Todoroki, S. Kimura, and K. Koike.** 2001. Oxidative stress in the absence of inflammation in a mouse model for hepatitis C virus-associated hepatocarcinogenesis. Cancer Res. **61**:4365–4370.
35. **Moriya, K., H. Yotsuyanagi, Y. Shintani, H. Fujie, K. Ishibashi, Y. Matsuura, T. Miyamura, and K. Koike.** 1997. Hepatitis C virus core protein induces hepatic steatosis in transgenic mice. J Gen. Virol. **78**:1527–1531.
36. **Murata, S., H. Kawahara, S. Tohma, K. Yamamoto, M. Kasahara, Y. Nabeshima, K. Tanaka, and T. Chiba.** 1999. Growth retardation in mice lacking the proteasome activator PA28gamma. J. Biol. Chem. **274**:38211–38215.
37. **Nelson, D. R., H. L. Lim, C. G. Marousis, J. W. Fang, G. L. Davis, L. Shen, M. S. Urdea, J. A. Kolberg, and J. Y. Lau.** 1997. Activation of tumor necrosis factor-alpha system in chronic hepatitis C virus infection. Dig. Dis. Sci. **42**:2487–2494.
38. **Niwa, H., K. Yamamura, and J. Miyazaki.** 1991. Efficient selection for high-expression transfectants with a novel eukaryotic vector. Gene **108**:193–199.
39. **Ogino, T., H. Fukuda, S. Imajoh-Ohmi, M. Kohara, and A. Nomoto.** 2004. Membrane binding properties and terminal residues of the mature hepatitis C virus capsid protein in insect cells. J. Virol. **78**:11766–11777.
40. **Okamoto, K., K. Moriishi, T. Miyamura, and Y. Matsuura.** 2004. Intramembrane proteolysis and endoplasmic reticulum retention of hepatitis C virus core protein. J. Virol. **78**:6370–6380.
41. **Okuda, M., K. Li, M. R. Beard, L. A. Showalter, F. Scholle, S. M. Lemon, and S. A. Weinman.** 2002. Mitochondrial injury, oxidative stress, and antioxidant gene expression are induced by hepatitis C virus core protein. Gastroenterology **122**:366–375.
42. **Ozes, O. N., H. Akca, L. D. Mayo, J. A. Gustin, T. Maehama, J. E. Dixon, and D. B. Donner.** 2001. A phosphatidylinositol 3-kinase/Akt/mTOR pathway mediates and PTEN antagonizes tumor necrosis factor inhibition of insulin signaling through insulin receptor substrate-1. Proc. Natl. Acad. Sci. USA **98**:4640–4645.
43. **Rui, L., T. L. Fisher, J. Thomas, and M. F. White.** 2001. Regulation of insulin/insulin-like growth factor-1 signaling by proteasome-mediated degradation of insulin receptor substrate-2. J. Biol. Chem. **276**:40362–40367.
44. **Shimoike, T., S. Mimori, H. Tani, Y. Matsuura, and T. Miyamura.** 1999. Interaction of hepatitis C virus core protein with viral sense RNA and suppression of its translation. J. Virol. **73**:9718–9725.
45. **Shimomura, I., R. E. Hammer, J. A. Richardson, S. Ikemoto, Y. Bashmakov, J. L. Goldstein, and M. S. Brown.** 1998. Insulin resistance and diabetes mellitus in transgenic mice expressing nuclear SREBP-1c in adipose tissue: model for congenital generalized lipodystrophy. Genes Dev. **12**:3182–3194.
46. **Shimomura, I., M. Matsuda, R. E. Hammer, Y. Bashmakov, M. S. Brown, and J. L. Goldstein.** 2000. Decreased IRS-2 and increased SREBP-1c lead to mixed insulin resistance and sensitivity in livers of lipodystrophic and ob/ob mice. Mol. Cell **6**:77–86.
47. **Shintani, Y., H. Fujie, H. Miyoshi, T. Tsutsumi, K. Tsukamoto, S. Kimura, K. Moriya, and K. Koike.** 2004. Hepatitis C virus infection and diabetes: direct involvement of the virus in the development of insulin resistance. Gastroenterology **126**:840–848.
48. **Shulman, G. I.** 2000. Cellular mechanisms of insulin resistance. J. Clin. Investig. **106**:171–176.
49. **Su, A. I., J. P. Pezacki, L. Wodicka, A. D. Brideau, L. Supekova, R. Thimme, S. Wieland, J. Bukh, R. H. Purcell, P. G. Schultz, and F. V. Chisari.** 2002. Genomic analysis of the host response to hepatitis C virus infection. Proc. Natl. Acad. Sci. USA **99**:15669–15674.
50. **Sun, X. J., J. L. Goldberg, L. Y. Qiao, and J. J. Mitchell.** 1999. Insulin-induced insulin receptor substrate-1 degradation is mediated by the proteasome degradation pathway. Diabetes **48**:1359–1364.
51. **Suzuki, R., S. Sakamoto, T. Tsutsumi, A. Rikimaru, K. Tanaka, T. Shimoike, K. Moriishi, T. Iwasaki, K. Mizumoto, Y. Matsuura, T. Miyamura, and T. Suzuki.** 2005. Molecular determinants for subcellular localization of hepatitis C virus core protein. J. Virol. **79**:1271–1281.
52. **Tamemoto, H., T. Kadowaki, K. Tobe, T. Yagi, H. Sakura, T. Hayakawa, Y. Terauchi, K. Ueki, Y. Kaburagi, S. Satoh, et al.** 1994. Insulin resistance and growth retardation in mice lacking insulin receptor substrate-1. Nature **372**: 182–186.
53. **Taniguchi, C. M., K. Ueki, and R. Kahn.** 2005. Complementary roles of IRS-1 and IRS-2 in the hepatic regulation of metabolism. J. Clin. Investig. **115**:718–727.
54. **Uysal, K. T., S. M. Wiesbrock, M. W. Marino, and G. S. Hotamisligil.** 1997. Protection from obesity-induced insulin resistance in mice lacking TNF-alpha function. Nature **389**:610–614.
55. **Vanhaesebroeck, B., and D. R. Alessi.** 2000. The PI3K-PDK1 connection: more than just a road to PKB. Biochem. J. **346**:561–576.

56. **White, M. F.** 1998. The IRS-signalling system: a network of docking proteins that mediate insulin action. Mol. Cell. Biochem. **182**:3–11.
57. **Withers, D. J., J. S. Gutierrez, H. Towery, D. J. Burks, J. M. Ren, S. Previs, Y. Zhang, D. Bernal, S. Pons, G. I. Shulman, S. Bonner-Weir, and M. F. White.** 1998. Disruption of IRS-2 causes type 2 diabetes in mice. Nature **391**:900–904.
58. **Yu, C., Y. Chen, G. W. Cline, D. Zhang, H. Zong, Y. Wang, R. Bergeron, J. K. Kim, S. W. Cushman, G. J. Cooney, B. Atcheson, M. F. White, E. W. Kraegen, and G. I. Shulman.** 2002. Mechanism by which fatty acids inhibit insulin activation of insulin receptor substrate-1 (IRS-1)-associated phosphatidylinositol 3-kinase activity in muscle. J. Biol. Chem. **277**: 50230–50236.

JOURNAL OF VIROLOGY, Feb. 2007, p. 1727–1735 Vol. 81, No. 4
0022-538X/07/$08.00+0 doi:10.1128/JVI.01683-06

Involvement of the PA28γ-Dependent Pathway in Insulin Resistance Induced by Hepatitis C Virus Core Protein[▽]

Hironobu Miyamoto,[1] Kohji Moriishi,[1] Kyoji Moriya,[2] Shigeo Murata,[3] Keiji Tanaka,[3] Tetsuro Suzuki,[4] Tatsuo Miyamura,[4] Kazuhiko Koike,[2] and Yoshiharu Matsuura[1]*

Department of Molecular Virology, Research Institute for Microbial Diseases, Osaka University, Osaka,[1] Department of Internal Medicine, Graduate School of Medicine, University of Tokyo, Tokyo,[2] Department of Molecular Oncology, Tokyo Metropolitan Institute of Medical Science, Tokyo,[3] and Department of Virology II, National Institute of Infectious Diseases, Tokyo,[4] Japan

Received 4 August 2006/Accepted 16 November 2006

The hepatitis C virus (HCV) core protein is a component of nucleocapsids and a pathogenic factor for hepatitis C. Several epidemiological and experimental studies have suggested that HCV infection is associated with insulin resistance, leading to type 2 diabetes. We have previously reported that HCV core gene-transgenic (PA28γ$^{+/+}$CoreTg) mice develop marked insulin resistance and that the HCV core protein is degraded in the nucleus through a PA28γ-dependent pathway. In this study, we examined whether PA28γ is required for HCV core-induced insulin resistance in vivo. HCV core gene-transgenic mice lacking the PA28γ gene (PA28γ$^{-/-}$CoreTg) were prepared by mating of PA28γ$^{+/+}$CoreTg with PA28γ-knockout mice. Although there was no significant difference in the glucose tolerance test results among the mice, the insulin sensitivity in PA28γ$^{-/-}$CoreTg mice was recovered to a normal level in the insulin tolerance test. Tyrosine phosphorylation of insulin receptor substrate 1 (IRS1), production of IRS2, and phosphorylation of Akt were suppressed in the livers of PA28γ$^{+/+}$CoreTg mice in response to insulin stimulation, whereas they were restored in the livers of PA28γ$^{-/-}$CoreTg mice. Furthermore, activation of the tumor necrosis factor alpha promoter in human liver cell lines or mice by the HCV core protein was suppressed by the knockdown or knockout of the PA28γ gene. These results suggest that the HCV core protein suppresses insulin signaling through a PA28γ-dependent pathway.

Hepatitis C virus (HCV) is the causative agent in most cases of acute and chronic non-A, non-B hepatitis (15). Over one-half of patients with the acute infection evolve into a persistent carrier state (24). Chronic infection with HCV frequently induces hepatic steatosis, cirrhosis, and eventually hepatocellular carcinoma (22) and is known to be associated with diseases of extrahepatic organs, including an essential mixed cryoglobulinemia, porphyria cutanea tarda, membranoproliferative glomerulonephritis, and type 2 diabetes (13).

HCV is classified into the genus *Hepacivirus* of the family *Flaviviridae* and possesses a viral genome consisting of a single positive-strand RNA with a nucleotide length of about 9.5 kb. This viral genome encodes a single polyprotein composed of approximately 3,000 amino acids (9). The polyprotein is post-translationally cleaved by host cellular peptidases and viral proteases, resulting in 10 viral proteins (6, 10, 12). The HCV core protein is known to interact with viral-sense RNA of HCV to form the viral nucleocapsid (44). The HCV core protein is cleaved off at residue 191 by the host signal peptidase to release it from the E1 envelope protein and then by the host signal peptide peptidase at around amino acid residues 177 to 179 within the C-terminal transmembrane region (30, 39, 40). The mature core protein is retained mainly on the endoplasmic reticulum, although a portion moves to the nucleus and mitochondria (11, 51).

Recent epidemiological studies have indicated that type 2 diabetes is an HCV-associated disease (7, 29). However, it remains unclear how insulin resistance is induced in patients chronically infected with HCV, since there is no suitable model for investigating HCV pathogenesis. Type 2 diabetes is a complex, multisystemic disease with pathophysiology that includes a high level of hepatic glucose production and insulin resistance, which contribute to the development of hyperglycemia (8, 18). Although the precise mechanism by which these factors contribute to the induction of insulin resistance is difficult to understand, a high level of insulin production by pancreatic β cells under a state of insulin resistance is common in the development of type 2 diabetes. The hyperinsulinemia in the fasting state that is observed relatively early in type 2 diabetes is considered to be a secondary response that compensates for the insulin resistance (8, 18).

The HCV core protein is also known as a pathogenic factor that induces steatosis and hepatocellular carcinoma in mice (33, 35). Previously, we reported that insulin resistance occurs in HCV core gene-transgenic mice due at least partly to an increase in tumor necrosis factor alpha (TNF-α) secretion (47) and that the HCV core protein is degraded through a PA28γ/REGγ (11S regulator)-dependent pathway in the nucleus (32). It is well known that PA28γ enhances latent proteasome activity, although the biological significance of PA28γ is largely unknown, with the exception that PA28γ is known to regulate steroid receptor coactivator 3 (28). Although several reports suggested that the degradation of insulin receptor substrate (IRS) proteins by a ubiquitin-dependent proteasome activity contributes to insulin resistance (43, 50), the involvement of the HCV core protein in cooperation with PA28γ in the stability of IRS proteins and in the development of insulin resis-

* Corresponding author. Mailing address: Department of Molecular Virology, Research Institute for Microbial Diseases, Osaka University, 3-1 Yamadaoka, Suita, Osaka 565-0871, Japan. Phone: 81-6-6879-8340. Fax: 81-6-6879-8269. E-mail: matsuura@biken.osaka-u.ac.jp.

[▽] Published ahead of print on 29 November 2006.

tance is not known. In this study, we examined the involvement of PA28γ in the induction of insulin resistance by the HCV core protein in vivo.

MATERIALS AND METHODS

Preparation of PA28γ-knockout HCV core gene-transgenic mice. C57BL/6 mice carrying the gene encoding HCV core protein genotype 1b ($PA28\gamma^{+/+}$ CoreTg) line C49 and $PA28\gamma^{-/-}$ mice have been described previously (35, 36). These two genotypes were crossbred to create $PA28\gamma^{+/-}$CoreTg mice. $PA28\gamma^{+/-}$CoreTg mice were bred to generate $PA28\gamma^{-/-}$CoreTg mice (35, 36). The HCV core gene and the target sequence to knock out the PA28γ gene were identified by PCR. The mice were given ordinary feed (CRF-1; Charles River Laboratories, Yokohama, Japan) and were maintained under specific-pathogen-free conditions.

Glucose tolerance test. The mice were fasted for more than 16 h before glucose administration. D-Glucose (1 g/kg body weight) was intraperitoneally administered to the mice. Blood samples were taken from the orbital sinus at the indicated time points. The plasma glucose concentration was measured by means of a MEDI-SAFE Mini blood glucose monitor (TERUMO, Tokyo, Japan). The serum insulin level was determined by a Mercodia (Uppsala, Sweden) ultrasensitive mouse insulin enzyme-linked immunosorbent assay (ELISA).

Insulin tolerance test. The mice were fed freely and then fasted during the study period. Human insulin (2 U/kg body weight) (Humulin; Eli Lilly, Indianapolis, IN) was intraperitoneally administered to the mice. The plasma glucose concentration was measured at the indicated time and was normalized based on the glucose concentration at the time just before insulin administration.

Histological analysis of pancreatic islets. Pancreas tissues were fixed with paraformaldehyde, embedded in paraffin, sectioned, and stained with hematoxylin and eosin. The relative islet area and islet number were determined with Image-Pro PLUS image analyzing software (NIPPON ROPER, Tokyo, Japan).

Estimation of tumor necrosis factor alpha and HCV core protein. Mouse TNF-α was measured by using a mouse TNF-α ELISA kit (Pierce, Rockford, IL) and normalized based on the amount of total protein in each sample. The protein concentration was estimated by using a BCA protein assay kit (Pierce). The amount of HCV core protein in the liver tissues was determined by using an ELISA system as described previously (4).

In vivo insulin stimulation and immunoblot analysis. Mice were fasted for more than 16 h before insulin stimulation and then anesthetized with ketamine and xylazine. Five units of insulin were injected into the mice via the interior vena cava. Livers of the mice were collected 5 min after the insulin injection and frozen in liquid nitrogen. Immunoblot analyses of the HCV core protein, PA28γ, and each of the insulin-signaling molecules were carried out with the liver tissue homogenates prepared in the homogenizing buffer containing 25 mM Tris-HCl (pH 7.4), 10 mM Na_3VO_4, 100 mM NaF, 50 mM $Na_4P_2O_7$, 10 mM EGTA, 10 mM EDTA, 2 mM phenylmethylsulfonyl fluoride, and 1% Nonidet P40 supplemented with Complete Protease Inhibitor Cocktail (Roche Diagnostics, Mannheim, Germany) (53). Tissue lysates were subjected to sodium dodecyl sulfate–2% to 15% gradient polyacrylamide gel electrophoresis (PAG Mini DAIICHI 2/15 13W; Daiichi Diagnostics, Tokyo, Japan) and electrotransferred onto polyvinylidene difluoride membranes (Immobilon-P; Millipore, Bedford, MA). The protein transferred onto the membrane was reacted with rabbit anti-HCV core (32), rabbit anti-Akt (Cell Signaling, Danvers, MA), rabbit anti-phospho-Ser473-Akt (Cell Signaling), rabbit anti-IRS1 (Upstate, Lake Placid, NY), rabbit anti-phospho-Tyr608 mouse insulin receptor substrate 1 (Sigma, St. Louis, MO), or rabbit anti-IRS2 (Upstate) polyclonal antibody and then incubated with horseradish peroxidase-conjugated anti-rabbit antibody. Blotted protein was visualized using Super Signal Femto (Pierce) and an LAS3000 imaging system (Fuji Photo Film, Tokyo, Japan).

Quantitative reverse transcription-PCR (RT-PCR). Total RNA was isolated from mouse liver using an RNeasy kit (QIAGEN, Valencia, CA). The RNA preparation was treated with a TURBO DNA-free kit (Ambion, Austin, TX) to remove DNA contamination in the samples. The first-strand cDNAs were synthesized by a first-strand cDNA synthesis kit (Amersham Biosciences, Franklin Lakes, NJ). The targeted cDNA was estimated by using Platinum SYBR Green qPCR Super Mix UDC (Invitrogen, Carlsbad, CA) according to the manufacturer's protocol. The fluorescent signal was measured by using an ABI Prism 7000 (Applied Biosystems, Foster City, CA). The genes encoding mouse TNF-α, IRS1, IRS2, and hypoxanthine phosphoribosyl transferase were amplified with the following primer pairs: 5′-GGTACAACCCATCGGCTGGCA-3′ (forward) and 5′-GCGACGTGGAACTGGCAGAAG-3′ (reverse) for TNF-α, 5′-ATAG CTCTGAGACCTTCTCAGCACCTAC-3′ (forward) and 5′-GGAGTTGCCCT CATTGCTGCCTAA-3′ (reverse) for IRS1, 5′-AGCCTGGGGATAATGGTG ACTATACCGA-3′ (forward) and 5′-TTGTGGGCAAAGGATGGGGACAC T-3′ (reverse) for IRS2, and 5′-CCAGCAAGCTTGCAACCTTAACCA-3′ (forward) and 5′-GTAATGATCAGTCAACGGGGGAC-3′ (reverse) for hypoxanthine phosphoribosyl transferase. Each PCR product was found as a single band with the correct size by agarose gel electrophoresis (data not shown).

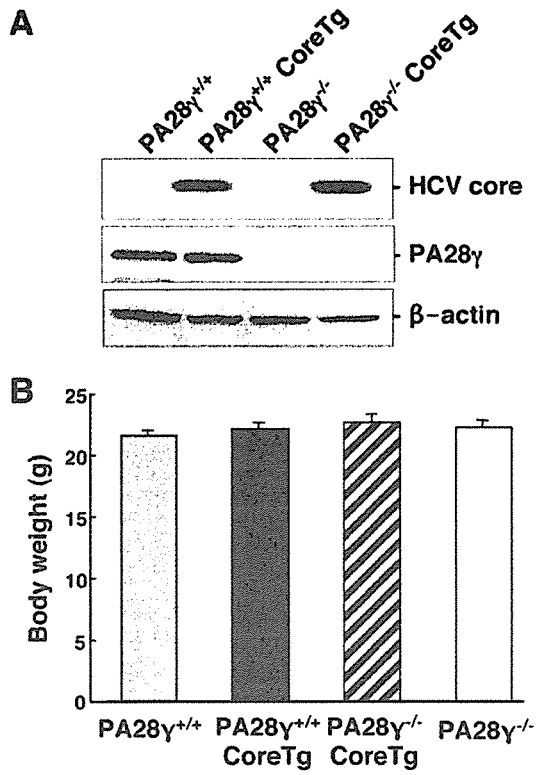

FIG. 1. Characterization of HCV core gene-transgenic mice deficient in the PA28γ gene. (A) Expression of the HCV core protein and PA28γ in the livers of $PA28\gamma^{+/+}$, $PA28\gamma^{+/+}$CoreTg, $PA28\gamma^{-/-}$, and $PA28\gamma^{-/-}$CoreTg mice. Lysates obtained from liver tissues of the mice (100 μg protein/lane) were subjected to sodium dodecyl sulfate-polyacrylamide gel electrophoresis and immunoblotting using antibodies to the HCV core protein, PA28γ, and β-actin. (B) Body weights of the mice. Body weights of 2-month-old mice were measured ($n = 7$ in each group). There were no statistically significant differences in body weights among the mice ($P > 0.05$).

Reporter assay for TNF-α promoter activity. The promoter region of the TNF-α gene (located from residues −1260 to +140) was amplified from mouse genomic DNA and was then introduced into the KpnI and BglII sites of pGL3-Basic (Promega, Madison, WI) (25). The resulting plasmid was designated as pGL3-tnf-aPro. The gene encoding the HCV core protein was amplified from HCV strain J1 (genotype 1b) and cloned into pCAG-GS (1, 38). To avoid contamination with endotoxin from *Escherichia coli*, the plasmid DNA was purified by using an EndoFree Plasmid Maxi kit (QIAGEN). The total amount of transfected DNA was normalized by the addition of empty plasmids. Plasmid vector was transfected into hepatoma cell lines by lipofection using Lipofectamine 2000 (Invitrogen). Cells were harvested at 24 h posttransfection. Luciferase activity was determined by using the Dual-Luciferase Reporter Assay system (Promega). Firefly luciferase activity was normalized to coexpressed *Renilla* luciferase activity. The amount of firefly luciferase activity was presented as the increase (n-fold) relative to the value for the sample lacking the HCV core protein, which was taken to be 1.0. PA28γ-knockdown cell lines were established by using pSilencer 2.1 U6 Hygro (Ambion) according to the manufacturer's protocol.

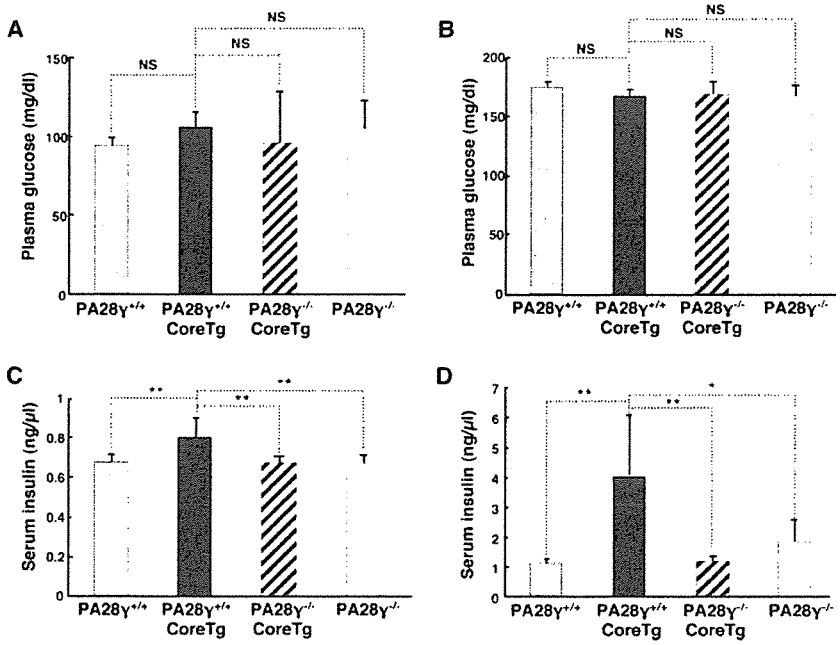

FIG. 2. Knockout of the PA28γ gene inhibited the hyperinsulinemia induced by HCV core protein. Plasma glucose levels of PA28$\gamma^{+/+}$, PA28$\gamma^{+/+}$CoreTg, PA28$\gamma^{-/-}$CoreTg, and PA28$\gamma^{-/-}$ mice under fasting (A) or fed (B) conditions (n = 7 in each group) are shown. Serum insulin levels in fasting (C) or fed (D) mice (n = 7 in each group) are also shown. Values are represented as means ± standard deviations. *P < 0.05; **P < 0.01. NS, not statistically significant.

Statistical analysis. The results are presented as means ± standard deviations. The significance of the differences was determined by Student's t test. P values of <0.05 were considered statistically significant.

RESULTS

HCV core gene-transgenic mice deficient in the PA28γ gene. To investigate the role of PA28γ in the development of insulin resistance in HCV core gene-transgenic (PA28$\gamma^{+/+}$CoreTg) mice, we generated HCV core gene-transgenic mice deficient in the PA28γ gene (PA28$\gamma^{-/-}$CoreTg). A PA28$\gamma^{+/+}$CoreTg mouse expressing an amount of PA28γ equal to that of its normal littermates (Fig. 1A) was crossbred with a PA28$\gamma^{-/-}$ mouse to generate a PA28$\gamma^{+/-}$ CoreTg mouse. PA28$\gamma^{+/-}$ CoreTg mice were bred with each other, and a PA28$\gamma^{-/-}$ CoreTg mouse was selected by PCR. The HCV core protein was expressed in PA28$\gamma^{+/+}$CoreTg and PA28$\gamma^{-/-}$CoreTg

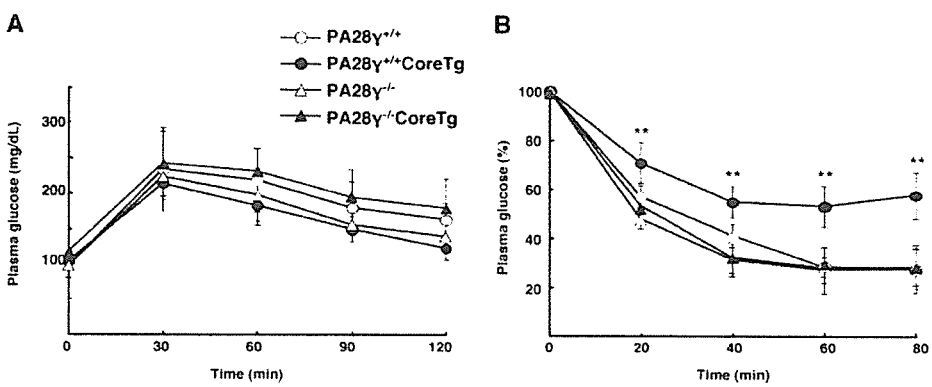

FIG. 3. Knockout of the PA28γ gene inhibits the insulin resistance induced by the HCV core protein. (A) Glucose tolerance test. D-Glucose was intraperitoneally administered to mice fasted for more than 16 h at 1 g/kg of body weight. Plasma glucose levels were estimated at the indicated times (n = 5 in each group). There were no significant differences in glucose levels among the mice (P > 0.05). (B) Insulin tolerance test. Human insulin (2 units/kg body weight) was intraperitoneally administered to the mice, and the plasma glucose levels were estimated at the indicated times. Values were normalized to the baseline glucose concentration at the time of insulin administration (n = 5 in each group). The values for the PA28$\gamma^{+/+}$ (open circles), PA28$\gamma^{+/+}$CoreTg (closed circles), PA28$\gamma^{-/-}$ (open triangles), and PA28$\gamma^{-/-}$CoreTg (closed triangles) mice are represented as means and ± standard deviations. Significant differences in insulin sensitivity (P < 0.01) in PA28$\gamma^{+/+}$CoreTg mice compared to that in PA28$\gamma^{+/+}$, PA28$\gamma^{-/-}$, or PA28$\gamma^{-/-}$CoreTg mice are indicated by double asterisks (**). There were no significant differences among PA28$\gamma^{+/+}$, PA28$\gamma^{-/-}$, and PA28$\gamma^{-/-}$CoreTg mice (P > 0.05).

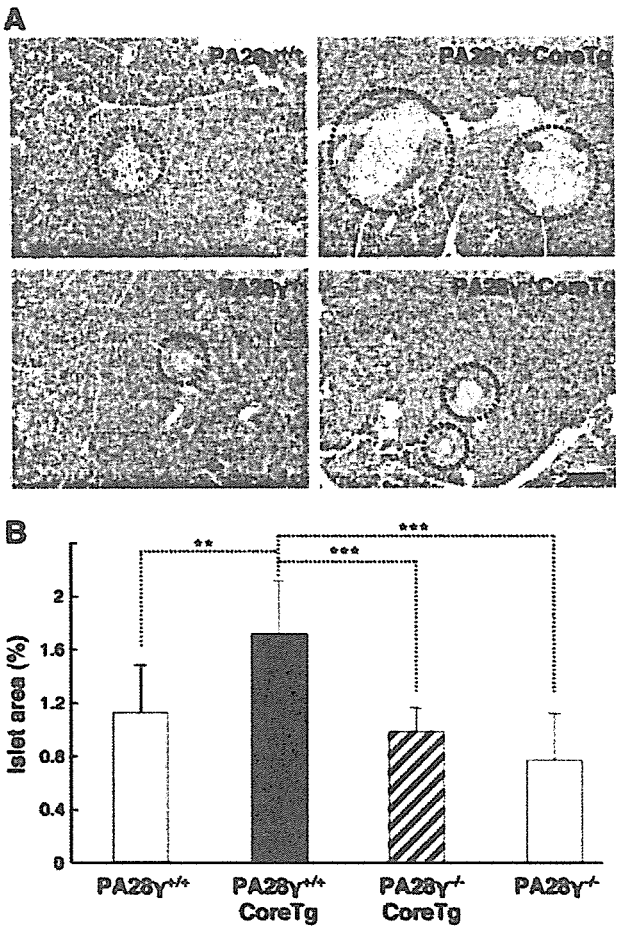

FIG. 4. PA28γ participated in the enlargement of pancreatic islets induced by the HCV core protein. (A) Histological sections prepared from pancreas tissues of PA28γ$^{+/+}$, PA28γ$^{+/+}$CoreTg, PA28γ$^{-/-}$, and PA28γ$^{-/-}$CoreTg mice were stained with hematoxylin and eosin. Dotted circles indicate pancreatic islets. (B) The area occupied by pancreatic islets was measured by computer software in three different fields of every six randomly selected sections of 10 mice per genotype and is represented as a percentage of the total pancreatic area. $**P < 0.01$; $***P < 0.001$. The scale bar indicates 100 μm.

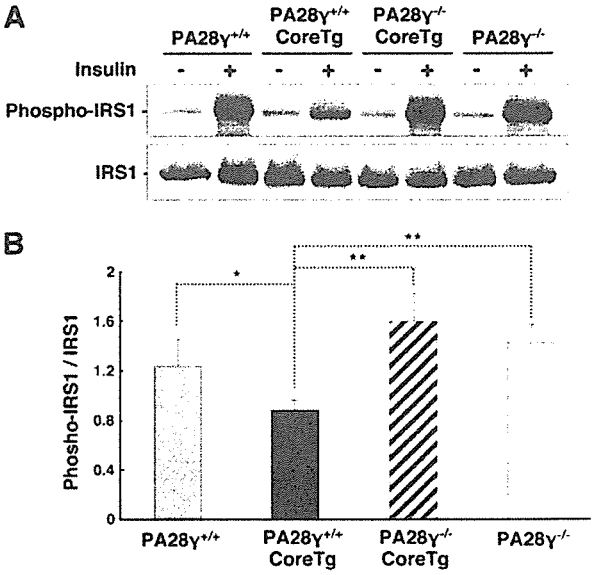

FIG. 5. PA28γ participated in the inhibition of the tyrosine phosphorylation of IRS1 induced by the HCV core protein. Liver tissues from PA28γ$^{+/+}$, PA28γ$^{+/+}$CoreTg, PA28γ$^{-/-}$, and PA28γ$^{-/-}$CoreTg mice were prepared after administration of insulin (+) or phosphate-buffered saline (−). The samples (100 μg of total protein) were examined by immunoblotting with antibodies against IRS1 and phospho-Tyr608 of mouse IRS1 (A). Phosphorylated IRS1 was estimated from the density on the immunoblotted membrane by using computer software (B) ($n = 5$ in each group). The data presented are representative of three independent experiments. $*P < 0.05$; $**P < 0.01$.

mice but not in PA28γ$^{+/+}$ (normal littermates) or PA28γ$^{-/-}$ mice. PA28γ was found at a similar level in PA28γ$^{+/+}$CoreTg and PA28γ$^{+/+}$ mice but was not present in either PA28γ$^{-/-}$ or PA28γ$^{-/-}$CoreTg mice (Fig. 1A). The expression of the HCV core protein in the livers of 2-month-old male mice was slightly higher in PA28γ$^{-/-}$CoreTg (1.36 ± 0.44 ng/mg of total protein; $n = 7$) than in PA28γ$^{+/+}$CoreTg (1.23 ± 0.22 ng/mg of total protein; $n = 7$) mice, but these values were not significantly different ($P > 0.05$). Insulin sensitivity is dependent on several conditions such as body weight, obesity, and liver steatosis (26). PA28γ$^{-/-}$ mice were slightly smaller than their normal littermates (PA28γ$^{+/+}$) at more than 3 months old, as described previously (36), but this was not significantly different in 2-month-old mice (Fig. 1B). PA28γ$^{+/+}$CoreTg mice exhibited severe hepatic steatosis from 4 months of age (35). To avoid the influence of hepatic steatosis and body weight on the examination of insulin resistance, 2-month-old mice were used in this study. Figure 1B shows the body weights of 2-month-old mice. There were no significant differences in body weight among PA28γ$^{+/+}$CoreTg, PA28γ$^{-/-}$CoreTg, PA28γ$^{-/-}$, and PA28γ$^{+/+}$ mice. Steatosis was not detected in the livers of the 2-month-old mice (data not shown).

PA28γ is involved in the development of hyperinsulinemia and insulin resistance in PA28γ$^{+/+}$CoreTg mice. In our previous study, we found a significant difference in serum insulin levels, but not in plasma glucose levels, between PA28γ$^{+/+}$ CoreTg mice and normal littermates (47). To determine the involvement of PA28γ in the development of insulin resistance in PA28γ$^{+/+}$CoreTg mice, we examined here the plasma glucose and insulin levels in the mice under fasting and fed conditions. Although no significant difference in plasma glucose levels was observed in the mice under either fasting (Fig. 2A) or fed (Fig. 2B) conditions, serum insulin levels were significantly higher in PA28γ$^{+/+}$CoreTg mice than in PA28γ$^{+/+}$ mice under both conditions (Fig. 2C and D), as described previously (47). In contrast, the serum insulin concentration in PA28γ$^{-/-}$CoreTg mice was recovered to a normal level similar to that of PA28γ$^{+/+}$ and PA28γ$^{-/-}$ mice under either fasting (Fig. 2C) or fed (Fig. 2D) conditions.

To determine the glucose intolerance among the mice, glucose was administered to the mice after fasting, and the plasma glucose level was then determined. There was no significant difference among the genotypes at any time point in the glucose tolerance test (Fig. 3A), suggesting that the volume of glucose was maintained at a normal level by the higher concentration of insulin in PA28γ$^{+/+}$CoreTg mice. In our previ-